Turbulent Airflow, Reynolds Stress, and Sand Transport Response over a Vegetated Foredune

by

Constance Alida Chapman
B.Sc., Simon Fraser University, 2009

A Thesis Submitted in Partial Fulfillment
of the Requirements for the Degree of

MASTER OF SCIENCE

in the Department of Geography

Supervisory Committee

Turbulent Airflow, Reynolds Stress, and Sand Transport Response over a Vegetated Foredune

by

Constance Alida Chapman
B.Sc., Simon Fraser University, 2009

Supervisory Committee

Dr. Ian J. Walker, **Supervisor**
(Department of Geography, University of Victoria)

Dr. Jody Klymak, **Outside Member**
(School of Earth and Ocean Sciences, University of Victoria)

Dr. Patrick A. Hesp, **Additional Member**
(Department of Geography and Anthropology, Louisiana State University)

Abstract

Supervisory Committee

Dr. Ian J. Walker, **Supervisor**
(Department of Geography, University of Victoria)

Dr. Jody Klymak, **Outside Member**
(School of Earth and Ocean Sciences, University of Victoria)

Dr. Patrick A. Hesp, **Additional Member**
(Department of Geography and Anthropology, Louisiana State University)

Recent research has revealed that quasi-instantaneous turbulent Reynolds stresses (RS, $-\rho u'w'$) and decomposed 'quadrant' activity (e.g., ejections and sweeps) over dunes in fluvial and wind tunnel studies has shown that turbulent stresses at the toe of a dune often exceed time-averaged, streamwise shear stress (ρu_*^2) estimates. It is believed that semi-coherent turbulent structures are conveyed toward the bed along concave streamlines in this region, and these activities cause fluctuations in local surface stresses that assist in grain entrainment. This study focuses on event-based landform scale interactions between turbulent airflow and sediment transport over a vegetated foredune through the assessment of two different experiments that took place at Greenwich Dunes, Prince Edward Island National Park, P.E.I., Canada. Reynolds decomposition of quasi-instantaneous fluctuating u' and w' signals into quadrant (Q) activity (i.e., Q1 outward interactions: $u'>0$, $w'>0$; Q2 ejections: $u'<0$, $w'>0$; Q3 inward interactions: $u'<0$, $w'<0$; Q4 sweeps: $u'>0$, $w'<0$) is explored to identify patterns of Reynolds stress signal distributions over the dune. Over flat surfaces, Q2 ejections and Q4 sweeps often dominate RS signals, whereas Q1 outward and Q3 inward interactions are less frequent

and contribute negatively to RS generation. Over dunes, however, topographically forced streamline curvature effects alter quadrant activity distributions and, hence, near-surface RS generation by enhancing (at the toe) or inhibiting (at the crest) turbulent motions. This results in Q2 ejection and Q4 sweep activity dominating stress generation on the beach, dune toe, and lower stoss slope, whereas, toward the crest, there is a shift toward Q1 outward and Q3 inward interactions. A flow 'exuberance effect' was identified that explains the contribution of positive to negative contributing activities that varies over the dune and helps explain the spatial pattern in RS. RS generation and sand transport depend on location over the dune (via topographic forcing effects on streamline curvature and flow stagnation/acceleration) and on incident flow direction via topographic steering effects that alter the apparent ‘steepness’ of the dune to flow streamlines. Transport on the lower portion of the dune was driven predominantly by ejection and sweep activity, while toward the crest it became dominated by outward and inward interactions, likely due to increased frequency of streamwise gusts (+u’) and vertical lift (+w’) in topographically compressed flow.

Table of Contents

List of Tables

List of Figures

Acknowledgments

I have very much enjoyed my Master's degree experience, and there are many people who have helped and supported me along the way. First of all, I would like to thank Dr. Ian J. Walker for his direction, support, and commitment. Thank you for providing me with the opportunity to go into the field on numerous occasions and for all the editorial feedback, which has allowed me to grow as a researcher immensely. It has been an absolute pleasure working with you! Thank you to Dr. Patrick Hesp, Dr. Robin Davidson-Arnott, Dr. Bernie Bauer, and Dr. Jeff Ollerhead for an amazing and unforgettable field experience and for all of the constructive criticism, suggestions, and support on the two manuscripts. Ian, Patrick, Robin, Bernie, and Jeff it has been a privilege to work with you all. BLASTer's thank you for all of your support. It has been a BLAST! Finally I would like to thank my wonderful family and friends. Dad, Mom, ACDC, thank you for always having the time to listen to me, for providing perspective, and supporting me unconditionally.

Thank you to all of you, I couldn't have done it without your help and support.

1.0 Introduction

1.1. Research Context

1.1.1. Importance of Beach-dune Systems

Coastal geomorphology explores how the processes of wind, wave, and current movements act on sediments to produce related landforms (Psuty, 2004). The most responsive coastal zones are typically areas that are wave dominated and have an abundance of sand supply (Short and Hesp, 1982; Psuty, 2004). Aeolian (windblown) sediment transport and dune formation is a function of the volume of available sand on the beach, the shape and width of the beach, and the nature of the wind regime (i.e., frequency, magnitude and directionality) (Short and Hesp, 1982; Psuty, 2004). Vegetation and other roughness elements (e.g., large woody debris, flotsam) in the backshore trap sand allowing for the formation and growth of foredunes. Beach-dune dynamics are a key factor in the classification of beaches (Short and Hesp, 1982). High-energy, dissipative beaches (i.e., high modal wave conditions and an abundant of sand supply) have the potential for the largest foredunes, which range from being stable, densely vegetated to unstable, sparsely vegetated, and hummocky (Short and Hesp, 1982; Hesp, 1988; Hesp, 2002). Reflective beaches (i.e., low modal wave conditions and sediment deficient surfzone) have small foredunes, whereas intermediate beaches (i.e., transitional features between dissipative and reflective beaches) has small to large foredunes (Short and Hesp, 1982). The wind regime ultimately controls beach-dune dynamics, sediment transport to the backshore and develop established foredunes, and the size of the dune (Short and Hesp, 1982). Greater onshore wind velocity increases the

potential for sediment transport to the backshore and foredunes. The orientation of the coastal beaches frequently determines the frequency of onshore winds influencing the amount of potential sediment transport (Short and Hesp, 1982). However, exposure to onshore winds is not the only factor for sediment transport, but beach morphology, gradient, and width are often more important in determining the rates of sediment transport (Short and Hesp, 1982). Sediment availability is one of the dominating variables that drives the development of the foredune characteristics, though it regularly depends on the transporting availability of the waves (Psuty, 2004).

Improved understanding of coastal dune dynamics is important in light of ongoing and future impacts of climate change and sea level rise. Foredunes often act as important buffers for backshore ecosystems and coastal towns to coastal erosion, storm surges, and gradual sea level rise. Beach-dune systems also provide important ecological functions as habitat for many different plants and animals. For example the dunes in Pacific Rim National Park Reserve of Canada on the west coast of Vancouver Island have endemic species (e.g., *Leymus mollis*), introduced/invasive species (e.g., *Ammophila breviligulata*, *Ammophila arenaria*), and threatened/endangered species (e.g., *Abronia umbellara*). Obtaining a greater understanding of dune dynamics will assist in and provide insight into dune erosion, re-building, and movement. This will aid in the advances of creating more realistic dune models and the planning and development of coastal towns with in dune systems.

1.1.2. Coastal Foredune Morphodynamics

The development and morphodynamics of sand dunes are controlled by fundamental interactions between fluid flow, dune morphology, and sediment transport (Walker and Nickling, 2002). Sediment transport depends on the frequency and magnitude of the fluid flow (wind regime) (Walker and Nickling, 2002). Changes in the fluid dynamics will result in sediment erosion, transport, and deposition, which allow for the development of bedforms and ultimately changes the dune morphology (Walker and Nickling, 2002).

In coastal settings, additional factors controlling dune development include: (1) sand supply; (2) vegetation type, cover and density; (3) rate of aeolian sand accretion and/or erosion; (5) frequency, magnitude and directionality of transporting winds; (6) the occurrence and magnitude of storm erosion, dune scarping, and overwash processes; (7) medium to long term beach or barrier state; (8) sea/lake/estuary water level; (9) extent of human impact and use (Hesp, 2002). Sand supply describes the amount of sand stored within the beach face and backshore and that is readily available to be transported and deposited on the lower stoss of the foredune or in the incipient foredune zone (Hesp, 1988). Vegetation density and type determine the amount of dune stabilization, where the vegetation density and type along with dune height indicates the location of sediment deposition (e.g., a densely vegetated dune has a greater potential for sediment to be deposited on the lower stoss) (Hesp, 1983; Hesp, 1988). Generally, the more frequent a beach experiences onshore winds, the greater the potential for sediment transport and backshore deposition. Dune development depends on the orientation of the coastal and

beach settings (Short and Hesp, 1982) and other factors, such as, tide range, wave dominance, and beach width and gradient, (Short and Hesp, 1982). Coastal dune systems are found all over the Earth and are dynamic features that often consist of several components, including: incipient foredunes, established foredunes, blowouts, and foredune planes. Foredunes are defined as shore-parallel dune ridges that form along the backshore by aeolian sand deposition (Hesp, 1988; Hesp, 2002). Incipient foredunes are ephemeral or developing foredunes that form on the upper beach by sand deposition within clumps of vegetation, around individual plants, or in large woody debris deposits (Hesp, 2002). Foredunes frequently colonize by the growth and development of woody vegetation species; as theses species become densely vegetated the foredunes become more stable and complex (Olsen, 1958; Hesp, 1988; Hesp, 2002). The development of incipient foredunes to established foredunes depends on sand supply availability, the type and density of the plant cover, the rate of aeolian accretion and erosion, and the magnitude of the wind and wave regime (Short and Hesp, 1982; Hesp, 1988). Sparsely vegetated, hummocky foredunes often have erosional blowout features that, depending on their size and intensity and directionality of the wind regime, have the potential to develop into large scale parabolic dunes (Short and Hesp, 1982; Hesp, 1988).

The factors that shape coastal dunes are challenging to quantify. Coastal dunes have been studied through two different perspectives: 1) the micro-scale perspective, where dune forming processes lead to the development of landforms; or 2) the macro-scale perspective, where the dune is examined to reconstruct processes and environmental history (Sherman, 1995). Therefore, for a general coastal dune system the micro -scale consists of seconds to months and millimetres to tens of metres; the meso-scale consists

of months to decades and hundreds of metres to tens of kilometres; the macro-scale consists greater than a decade and more then tens of kilometres (Sherman, 1995). It is extremely challenging integrating the different scales into a single model. Due to this scaling problem, it is particularly difficult to provide or develop a process-based prediction of landform development for time periods such as, years to decades (Sherman, 1995).

Factors controlling dune dynamics and development are often measured at the micro-scale such as wind flow and sediment transport. Though, conceptual dune models predicting dune development are often presented at the meso-scale (Sherman, 1995). Due to this shift in scale there is often a loss in confidence in the model due to the scaling differences, making dune modelling extremely challenging (Sherman, 1995). When examining the relationship between different factors it must be noted that these factors through space and time with the variability of each increasing over time and many of them are co-dependent (Sherman, 1995).

Recent meso-scale modeling of dune fields has been relatively successful. Nield and Baas (2008a and 2008b) developed a model called the DECAL which, uses a cellular automaton modelling approach, has the capability of simulating vegetated dunes in coastal and semi- arid environments. This model stresses the relationship between multiple vegetation types and different sediment supply and transport rates (Nield and Baas, 2008a; Nield and Baas, 2008 b). The DECAL model has been useful in assessing qualitative trends in the medium to long term spatial and temporal variations in dune field behaviour (Nield and Baas, 2008b). It has been accurate in stimulating long term long

trends and vegetation cover that matches current stabilizing dune patterns (Nield and Baas, 2008b).

1.1.3. Boundary Layer Theory and Flow Dynamics over Dunes

The planetary or atmospheric boundary layer (PBL) is the layer of atmosphere that extends from the surface to about 1 km up in vertical thickness (Oke, 1978). The PBL is characterized by well developed mixing that is generated by frictional drag as the atmosphere moves across the rough and rigid surface of the Earth (Oke, 1978). The height of the boundary layer is not constant with time and it varies due to the strength of the surface generated mixing (Oke, 1978). The PBL can be divided up in to five main sub layers: 1) Outer layer, 2) Turbulent surface layer, 3) Roughness layer, 4) Laminar boundary layer, and 5) sub surface layer. The outer layer is the outer 90% of the PBL layer and the depth of it is not consistent throughout the day but depends on the amount of turbulence, surface roughness, flow speed, surface generated mixing, and convection (Oke, 1978). The turbulent surface layer or also known as the constant stress region is dominated by intense small scale turbulence generated by the surface roughness and convection (Oke, 1978). During the day the turbulent surface layer can extend to a height of about 50 m, but at night as the boundary layer depth shrinks it often becomes only a few meters in height (Oke, 1978). Typically this area is only 10 to 15% of the PBL and is often log linear allowing for the Law of the Wall to be used. The Law of the Wall indicates that during steady uniform flow the lower part of the time-averaged wind speed profile over a flat homogenous surface can be described by a log linear increase in velocity with height (Oke, 1978). The velocity profiles change in response to the level of

turbulence which depends on the nature of the surface, as well as the on the velocity outside the boundary layer. The roughness layer extends above the tops of the elements by 1 to 3 times their height or spacing and the flow in this region is highly irregular due to the effect of individual roughness features (e.g., trees, buildings, sand, grass) (Oke, 1978). The laminar layer is in direct contact with the surface and is the non-turbulent layer which extends in height only a few millimetres (Oke, 1978). This layer sticks to all surfaces creating a buffer between the surface and the diffusive environment (Oke, 1978). The laminar layer often experiences flow streamlines that are parallel and the flow is slow over flat, smooth, surfaces. The sub surface layer is a very thin layer where molecular exchange takes place (i.e., molecular viscosity). This layer is very thin and surrounds the individual surface roughness features, such as, each individual sand grain.

Complications in near-surface flow dynamics occur as boundary layer flow encounters dunes and hills resulting from changes in flow streamlines and pressure gradients that emerge. As flow approaches a dune or a hill there is a positive pressure build up or flow stagnation effect at the base of the dune, causing streamline concavity (Walker and Nickling, 2002). Along the stoss of the dune there is a negative pressure gradient and flow increases (Walker and Nickling, 2002). At the crest there is a drop in pressure as the flow is compressed and accelerated, resulting in streamline convexity (Walker and Nickling, 2002). The Jackson and Hunt (1975) model divides boundary layer flow over low hills into an outer and inner region. The outer layer is characterized by minimal turbulent momentum exchange and is unaffected by surface shearing forces (Walker and Nickling, 2002). The effects of turbulent momentum exchange and surface shear are significant in the inner region (Walker and Nickling, 2002). The inner region is

divided into two different layers, the inner surface layer (ISL) and the shear stress layer (SSL) (Jackson and Hunt, 1975). In the outer region, the flow is modified by the pressure field only, whereas, in the inner region the flow is characterized by turbulent momentum exchange and surface shear (Walker and Nickling, 2002). There are two different scales of surface roughness that flow encounters: i) skin friction also known as surface drag and ii) form roughness that is brought on by a slope and usually involves flow separation. Surface roughness (z_0) affects the flow especially as it moves from a relatively flat, open source, such as a lake or ocean, to the beach and over a vegetated dune or hill, as this occurs the boundary layer often goes through several transitions as each new roughness is encountered over the slope (Sherman and Bauer, 1993). As the roughness increases, flow speeds decrease in the layer just above the surface, gradually working its way up to higher levels (Olsen, 1958). The Jackson and Hunt (1975) model has been successful at advancing the predictability of the boundary layer theory for different topographical surfaces and atmospheric flows, though its ability to predict surface shear stress and sediment transport in the near surface boundary layer over dunes remains limited (Walker and Nickling, 2002). Instead, recent research has explored correlations between near-surface wind speeds and measured sediment flux in order to better understand flow-transport relations over dunes (e.g., Lancaster et al., 1996; Davidson- Arnott et al,. 2008, Bauer et al., 2009).

1.1.4. Surface Stress Characterization

Surface stress responsible for sediment transport can be quantified by two different methods: 1) the boundary layer theory, in which time-averaged velocity profiles

and the Law of the Wall equation are utilized, and 2) the turbulent Reynolds Stress (RS), in which a quasi-instantaneous vertical flux of the horizontal momentum at a point is derived using fluctuations of opposing streamwise (u') and vertical (w') velocity measurements is used.

The boundary layer theory explains the velocity profile over a surface and where the shear stress forms at the boundary. During steady, uniform flow conditions a constant shear stress layer exists within the inner region that displays a log-linear relationship in velocity with the height (Walker and Nickling, 2002). This phenomenon is known as *the Law of the Wall*. The logarithmic portion (i.e., constant stress region) of the boundary layer can be described by the Prandtl-von Karman equation:

$$\frac{u_z}{u_*} = \frac{1}{k}\left(ln\frac{z}{z_0}\right) \tag{1.1}$$

where u_z is the horizontal velocity (m/s), u_* is the shear velocity (m/s), z is the height (m), z_0 is the roughness length (m), and the k is the von Karman's constant (≈0.4). The surface shear stress τ_o cannot usually be measured directly in sedimentary environments and, thus, a shear velocity (u_*) term is often used to estimate the shear stress:

$$\tau_o = \rho_a {u_*}^2 \tag{1.2}$$

where τ_o is the shear stress, u_* is the shear velocity (m/s), and ρ_a is the air density. Often natural flow conditions (e.g., unsteady, multi-directional surface winds over rough surfaces) produce profiles that do not correspond with the log linear model (Walker and Nickling, 2002). However, this can often be resolved by using longer time-averaging intervals and or increasing the spatial resolution of measurements (Walker and Nickling, 2002).

Turbulent Reynolds stress (RS) quantifies a quasi-instantaneous, at-a-point estimate of the vertical flux of horizontal momentum produced by velocity fluctuations in the flow field. Statistically, RS is proportional to the covariance between orthogonal velocity components as characterized by deviations in horizontal (u') and vertical (w') planes with reference to their respective mean values. Though only one (u-w) of the three (u-v, w-v) Reynolds stress components is utilized and examined. The Reynolds stress equation is as follows:

$$RS = -\rho_a \overline{u'w'} \tag{1.3}$$

where ρ_a is fluid density and the over bar indicates a time average of the product of quasi-instantaneous velocity values. A kinematic Reynolds stress (RS_k) is often used and is defined as:

$$RS_k = -\overline{u'w'} \tag{1.4}$$

where the fluid density is removed.

1.1.5. Microturbulent Events and Near-surface Reynolds Stress Generation

Coherent micro turbulent structures consist of low speed streaks, hairpin vortices, ejections, and sweeps. Low speed streaks lift up growing/evolving into an ejection, which either acts independently or group together with other ejections to give rise to the boundary layer bursting (Jackson, 1976; Best, 1993). Ejections and subsequently bursts are known to have a hairpin or horse shoe vortex shape. It is thought that these hairpin vortices become stretched and elongated with higher Reynolds numbers (Jackson, 1976; Best, 1993). The sweep is the strong downward inrush of fluid and is thought to contribute a large portion of Reynolds stress within the flow (Jackson, 1976; Best, 1993).

Reynolds stresses can be decomposed into four different turbulent quadrant activities that are associated with the near-surface turbulent bursting process: i) quadrant 1 (Q1) outward interactions ($u'>0$, $w'>0$), ii) quadrant 2 (Q2) ejections ($u'<0$, $w'>0$), which is fluid moving away from the bed where compared to the mean value the vertical component is moving faster and the streamwise is moving slower, iii) quadrant 3 (Q3) inward interactions ($u'<0$, $w'<0$), and iv) quadrant 4 (Q4) sweeps $u'>0$, $w'<0$), strong inrush of fluid moving towards the bed where compared to the mean value the vertical component is moving slower and the streamwise is moving faster (Lu & Willmarth, 1973; Jackson, 1976). Upward quadrant 2 (ejections) and downward quadrant 4 (sweeps) contribute positively to RS and tend to dominate stress generation on flat surfaces and the lower stoss slope of a dune, whereas quadrant 1 (outward interactions) and quadrant 3 (inward interactions), that contribute negatively to RS generation, appear to dominate near surface stress toward the crest of the dune (Wiggs and Weaver, in review).

To date there is a limited understanding as to how turbulent airflow initiates sand transport over aeolian dunes. In contrast, fluvial research has identified that near-surface micro turbulence plays a significant role in saltation and suspended sediment entrainment and transport over sub-aqueous dunes (e.g., Jackson, 1976; Drake et al., 1988; Best 1993; Roberts et al., 1996; Venditti and Bennett, 2000; Best and Kostaschuk, 2002; Roy et al., 2004; Kostaschuk et al., 2008; Kostaschuk et al., 2009; Shugar et al., 2010). For instance, high RS stresses and associated quadrant activities (namely ejections and sweeps) have been associated with sediment entrainment and transport with buoyancy force playing a substantial role (Jackson, 1976; Drake et al., 1988; Best, 1993; Robert et al., 1996; Best and Kostaschuk, 2002; Roy et al., 2004; Kostaschuk et al., 2008; Kostaschuk et al., 2009;

Shugar et al., 2010). This is because buoyancy effects are in the order of magnitudes greater than air. For example the density of quartz is 2650 kg m^{-3} and air density at sea level is 1.23 kg m^{-3}, therefore the density ratio for sand in air is approximately 2155:1 vs. 2.65:1 in water at standard temperature and pressure. Coherent micro turbulent structures (e.g., low speed streaks, hairpin vortices, ejections, and sweeps) that exist in turbulent boundary layer flow generate high Reynolds stresses and contribute to sediment transport (Jackson, 1976; Best, 1993; Roy et al., 2004). Low speed streaks lift up growing/evolving into an ejection. The ejection either acts independently or groups together with other ejections to give rise to boundary layer bursting (Jackson, 1976; Best, 1993). The strong downward inrush of the fluid, known as a sweep, impinges the bed and entrains sediment at average rates and transports it at faster than average speeds (Drake et al., 1988; Best, 1993).

Recent wind tunnel research has shown that turbulent fluctuations in airflow at the toe of the dune often produce RS values that exceed time-averaged, streamwise shear stress (ρu_*^2) estimates (e.g., Wiggs et al., 1996; Walker and Nickling, 2002; 2003; Parsons et al., 2004). This results from turbulent structures that are conveyed toward the bed and are upwardly deflected (i.e., concave) streamlines. Toward the crest of a dune, surface stress often increases and is thought to be dominated by streamwise accelerations that result directly from streamline compression and suppression of turbulence via streamline convexity in this region (e.g., Wiggs et al., 1996; Walker and Nickling, 2002).

Changes in Reynolds stresses and flow properties are attributed to topographic forcing effects, where concave streamlines at the toe destabilizes the flow resulting in an increase in shear stress generation through the conveyance of turbulent structures towards

the bed (Wiggs et al., 1996; Walker and Nickling, 2002). Convex streamlines at the crest stabilizes the flow through the suppression of vertical motions (hinders the vertical velocity fluctuations w') (Wiggs et al., 1996; Walker and Nickling, 2002).

There is very little information on turbulent airflow, RS quadrant activity distributions, and sand transport responses over aeolian dunes. Recent work over barchan dunes in Namibia show that ejection and sweep activities dominate at the toe of the dune (Wiggs and Weaver, in review) and, while ejections are most frequent (occur about 1/3 of the time), sweeps are responsible for more then 2/3 of all the sediment transport (Wiggs and Weaver, in review). Toward the crest of the dune outward interactions and inward interactions dominate, where outward interactions were responsible for about 1/3 of the sediment transport (Wiggs and Weaver, in review). Weaver and Wiggs (2011) and Baddock et al., (2011) suggested that changes in turbulent structures may be caused by streamline curvature and deceleration/acceleration. Reynolds stress components at the toe of the dune were found to increase even as flow decreased, whereas, at the crest as flow increased there was a decrease in Reynolds stress (Weaver and Wiggs, 2011, Baddock et al., 2011). To date, the characterization and quantification of turbulent RS patterns and decomposed quadrant activity distributions is limited to this research and that presented in this thesis. Although widely used in fluvial and meteorological research, the characterization and quantification of turbulent RS and sand transport over a coastal dune system remains limited and poorly understood.

Other methods in the aeolian field have been utilized in order to explore Reynolds stresses and the relationship between turbulent airflow and sediment transport. The most common methods in the aeolian field are Reynolds rules of decomposition and spectral

descriptions and correlations (e.g., time series) (Bauer et al., 1998). An issue that has arisen when using these methods is that cup anemometers and 2-D sonic anemometers only provided a velocity (1-D component) and a velocity and direction (2-D components), therefore the focus of these methods has been on the velocity component, u. Recent development of technology now allows the streamwise, spanwise, and vertical velocity components to be measured. The Reynolds stress decomposition method and quadrant event method is utilized due to the effectiveness and that it allows simple visual comparisons, it shows the w' contributions, and relates easily to estimates of Reynolds stress.

1.1.6. Sediment Transport

With advances in instrumentation and questions regarding the role of turbulent velocity fluctuations in aeolian sediment transport (e.g., Walker 2005), there has been recent interest in exploring relations between turbulent airflow and sediment transport responses over dunes. Sediment transport over a beach and foredune is a complex, dynamic process controlled by how the wind field interacts with beach-dune geometry and slope, surface roughness conditions (e.g., grain size, bedforms, vegetation), sediment moisture content, and sediment supply (Bauer et al., 2009). When the sediment moisture content is highest there is a possibility that already saltating sand grains may adhere to the surface (Davidson-Arnott et al., 2008). In order to entrain sediment when moisture content is high a greater sediment transport threshold is required (Davidson-Arnott et al., 2008). Vegetation density plays a more substantial role in altering sediment supply to and transport over foredunes in comparison to vegetation type (Hesp, 1983). Dune height and

flow regime control the amount and location of deposition of sediment over the dune (Sarre, 1989; Arens, 1996). Sand on the beach is transported by saltation, but as it encounters the dune changes in roughness and topography generated turbulence modify and change the trajectories (Arens, 1996, Bauer et al., 2009). Sand transport on the beach is roughly three orders of magnitude greater than sand transport over the foredune (Arens, 1996). Arens (1996) proposed a conceptual model of four different scenarios for sediment transport and deposition during onshore flow for two different dune types: bare foredune and vegetated foredune. Focusing on just a vegetated foredune, when there are low wind speeds there is saltation occurring on the beach with potential for deposition at the toe of the dune (Arens, 1996). Over the stoss and crest of the foredune there is no potential for transport, deposition, or erosion (Arens, 1996). Whereas, for high wind speeds there is saltation occurring on the beach with suspension and deposition occurring at the crest (Arens, 1996). This conceptual model provides a basis as to how sand moves over a foredune and where the main areas of deposition tend to occur. A greater understanding of sediment transport will provide increased knowledge in sediment supply, pathways, and budgets allowing for increase awareness in dune growth, erosion and deposition.

1.1.7. Research Gap

This research focuses on event-based landform scale interactions between turbulent airflow and sediment transport over a vegetated foredune in an effort to improve the understanding of coastal dune morphodynamics. This research gap results, in part, from a delay in availability of turbulence instrumentation (Walker, 2005) and high-

resolution saltation sensors combined with the uncertainty of turbulence (notably, vertical velocity variations) in aeolian systems. Recent advances in, and increased availability of, robust, affordable, high- frequency turbulence instrumentation (e.g., ultrasonic anemometers, hot film probes) and sand transport measurement devices (e.g., saltation impact sensors, laser particle counters) has improved the ability to measure relations between turbulent near-surface airflow, shearing stresses and sediment transport over aeolian dunes (e.g., Wiggs et al., 1996; Walker and Nickling 2002, 2003; Baas, 2006; Livingstone et al., 2007; Walker et al., 2009a; Walker et al., 2009 b; Lynch et al., 2009; Weaver and Wiggs, 2011; Baddock et al. 2011; Wiggs and Weaver, in review).

1.2. Thesis Structure and Research Purpose and Objectives

This thesis is structured around two core results sections (2 and 3) derived from two discrete experiments in 2004 and 2010 over the same stretch of foredune in the Greenwich Dunes, Prince Edward Island National Park, Prince Edward Island, Canada. Each section is prepared as a research manuscript to be submitted to a peer-reviewed journal. These sections are bookended with an Introduction (Section 1.0) that sets the research context and a Summary and Conclusions (Section 4.0) section that reviews key findings of the research.

The general purpose of this thesis is to provide an improved understanding of the interactions between turbulent airflow and sediment transport over a vegetated foredune in an effort to improve the understanding of the morphodynamics of coastal foredunes. This purpose is explored through the following research objectives. Section 2.0 examines high frequency (32 Hz) measurements of three-dimensional turbulent velocity

components at four locations and two different sample heights over a vegetated foredune using the decomposed Reynolds stress and quadrant activity method. Specifically, the objectives of this paper are to:

1. To measure high-frequency variations in turbulent velocity components (i.e., u,v,w) at two different heights and four different locations over a vegetated foredune.
2. To quantify and examine patterns in, and properties of airflow behaviour and decomposed turbulent Reynolds stress signals that drive surface stress generation with a goal of improving understanding of aeolian sand transport process over foredunes.
3. To interpret interactions between turbulent flow, topographic forcing effects (e.g., streamline curvature and compression) and dune position, from this, dune morphodynamics are discussed.

Section 3.0 quantifies and explores coarser scale (1 Hz) interactions between turbulent airflow behaviour, Reynolds stress signal distribution, and sand transport over a vegetated foredune in order to expand on the findings on flow dynamics (Section 2.0). Specific objectives of this section include:

1. To measure variations in quasi-instantaneous (1hz) near-surface three-dimensional velocity components (i.e., u, v, w) and co-located sand transport intensity (grain counts) along a transect over a coastal foredune.

2. To examine relationships between near-surface airflow, decomposed quadrant activity structures (e.g., ejections, sweeps, inward/outward interactions) responsible for Reynolds stress generation and coincident sand transport.
3. To explain patterns in near-surface airflow dynamics, RS signal distribution and observed sand transport.
4. To discuss implications for sand supply and transport patterns over a vegetated foredune.

2.0. Turbulent Reynolds Stress and Quadrant Activity Behaviour over a Vegetated Foredune

2.1. Abstract

Recent research on quasi-instantaneous turbulent Reynolds stresses (RS, $-\rho u'w'$) and decomposed 'quadrant' activity (e.g., ejections and sweeps) over dunes in fluvial settings and in wind tunnels has shown that turbulent stresses at the toe of a dune often exceed time-averaged, streamwise shear stress (ρu_*^2) estimates. It is believed that semi-coherent turbulent structures are conveyed toward the bed along concave streamlines in this region, and these activities cause fluctuations in local surface stresses that assist in grain entrainment. This may explain how sand is supplied to the windward slope through a region of possible flow stagnation. Toward the crest, surface stress increases and becomes dominated by streamwise accelerations resulting from streamline compression and convexity that suppress vertical motions.

High-frequency (32 Hz) measurements of turbulent wind flow from 3-D ultrasonic anemometry are analyzed for oblique onshore flow over a vegetated foredune in Prince Edward Island, Canada. Reynolds stress and quadrant activity distributions varied with height (0.60 m and 1.66 m) and location over the dune. In general, quadrant 2 ejection ($u'<0, w'>0$) and quadrant 4 sweep activities ($u'>0, w'<0$) dominate momentum transfer and Reynolds stress generation over quadrant 1 outward interaction ($u'>0, w'>0$) and quadrant 3 inward interaction ($u'<0, w'<0$). On the lower stoss slope, ejection and sweep activities were most frequent (63 to 67%, ejections plus sweeps), whereas, at the crest, ejection and sweep activities became less frequent while outward and inward

interactions increased in frequency (40-45%). An ‘exuberance effect’ (i.e., changing shape of quadrant frequency distribution skewed toward ejection and sweep activity) is observed whereby streamline compression and convexity effects and inhibit vertical fluctuations in flow and, thus, reduce the frequency of ejections and sweep activity toward the crest. In the separated lee-side eddy behind the crest, quadrant distributions were more symmetrical as a result of more mixed, multi-directional flow behaviour. These trends in the structure of turbulence and in average shear stress have implications for sediment transport dynamics across the dune and may help to explain dune form maintenance. For example, areas experiencing a high frequency of ejection and sweep activity may have a high rate of sediment entrainment and transport, whereas areas experiencing a decline in ejection and sweep activity and an increase in outward and inward interactions may experience greater amounts of deposition.

2.2. Introduction

Research on quasi-instantaneous turbulent Reynolds stresses and decomposed ‘quadrant’ activities (e.g., ejections and sweeps) associated with turbulent near-surface shearing flow over aeolian dunes lags behind the research undertaken in fluvial settings (e.g., Drake et al., 1988; Roy et al., 1996; Walker, 2005; Wiggs and Weaver, in review). In recent years, a significant amount of research has been conducted on how dune forms interact with and may be maintained by fluid flow and how sediment is transported in the flow stagnation zone at the upwind base of the dune. Recent wind tunnel research has shown that turbulent Reynolds stresses at the toe of a dune often exceed time-averaged, streamwise shear stress (ρu_*^2) estimates (e.g., Wiggs et al., 1996; Walker and Nickling,

2002; 2003; Parsons et al., 2004). It is widely appreciated that turbulent Reynolds stresses have been associated with saltation and suspended sediment entrainment processes (Jackson, 1976; Drake et al., 1988; Best, 1993; Robert et al., 1996, Best and Kostaschuk, 2002; Roy et al., 2004; Kostaschuk et al., 2008; Kostaschuk et al., 2009; Shugar et al., 2010) and this may explain how sand can be supplied from the beach to the stoss slope of a foredune through a region of possible flow stagnation at the dune toe. The majority of the fluvial research has been focused on suspended sediment (e.g., Jackson, 1976; Best, 1993; Robert et al., 1996, Best and Kostaschuk, 2002; Roy et al., 2004, Kostaschuk et al., 2008; Kostaschuk et al., 2009; Shugar et al., 2010) with a couple focused on saltation of the bedload (e.g., Drake et al., 1988; Valyrakis et al., 2010), Through these findings it many help to explain the transport and entrainment of sand over the dune in both saltation and modified suspension.

Turbulent quadrant activities are characterized by quasi-instantaneous deviations in horizontal (u) and vertical (w) velocity components about their respective mean values (U, W) (Figure 2.1), such that:

$$u' = u - U \tag{2.1}$$

$$w' = w - W \tag{2.2}$$

where prime values indicated fluctuating components of horizontal (u') and vertical (w') velocity. These values are used to quantify turbulent Reynolds stress (RS) as follows:

$$RS = -\rho_a \overline{u'w'} \tag{2.3}$$

where ρ_a is air density and the over bar indicates a time average of the product of quasi-instantaneous velocity values. A kinematic Reynolds stress (RS_k) is often defined as:

$$RS_k = -\overline{u'w'} \tag{2.4}$$

Reynolds stress is commonly interpreted as the time-averaged vertical flux of horizontal momentum at a point produced by fluctuations in a flow field. In a statistical sense, the kinematic Reynolds stress is proportional to a covariance between orthogonal velocity components.

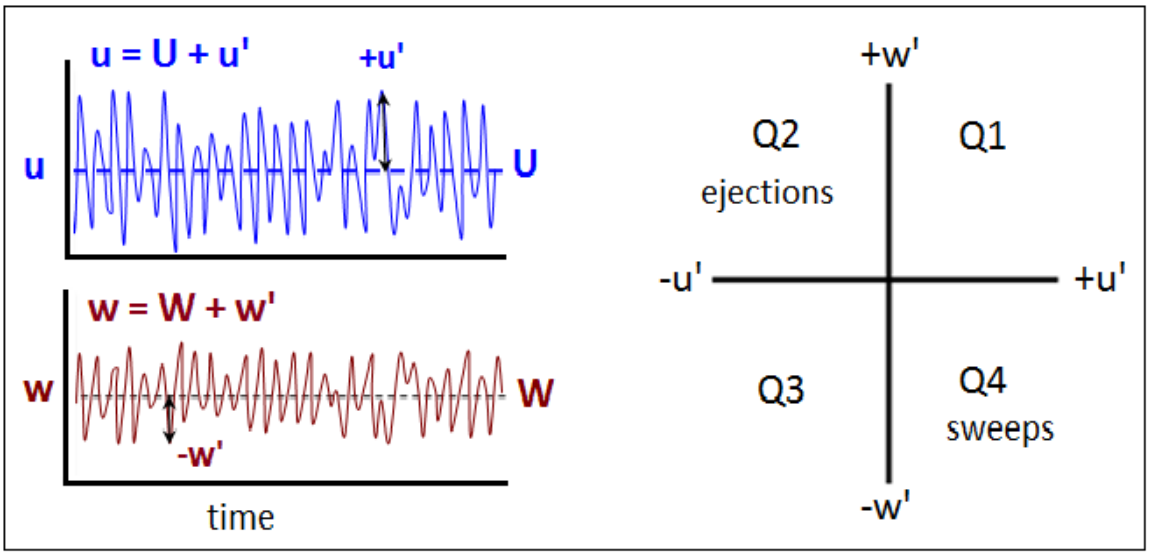

Figure 2.1: Turbulent velocity time series components plotted as quasi- instantaneous u' and w' quadrants where Q2 and Q4 activity typically dominate the Reynolds stress signal.

Reynolds stress signals can be decomposed into four categorical activities that are associated with the near-surface turbulent bursting process: i) quadrant 1 (Q1) outward interactions ($u'>0$, $w'>0$), ii) quadrant 2 (Q2) ejections ($u'<0$, $w'>0$), which is fluid moving away from the bed where compared to the mean value the vertical component is moving faster and the streamwise is moving slower, iii) quadrant 3 (Q3) inward interactions ($u'<0$, $w'<0$), and iv) quadrant 4 (Q4) sweeps ($u'>0$, $w'<0$), strong inrush of fluid moving towards the bed where compared to the mean value the vertical component is moving slower and the streamwise is moving faster (Figure 2.1) (Lu and Willmarth, 1973; Jackson, 1976). Upward ejections (Q2) and downward sweeps (Q4) tend to dominate Reynolds stress generation in turbulent boundary layers subject to fluid shear above relatively flat surfaces (Jackson, 1976). These 'activities' contribute positively to Reynolds stress generation and are thought to play a significant role in sediment entrainment and transport over bedforms (e.g., Jackson, 1976; Drake et al., 1988; Robert et al., 1996; Best, 1993; Roy et al., 2004; Kostaschuk et al., 2008; Kostaschuk et al., 2009; Shugar et al., 2010) and in momentum exchange above vegetation canopies (e.g., Lee and Black, 1993; Yue et al., 2007; Finnigan et al., 2009; Mazumder et al., 2009; Nemitz et al., 2009; Nemitz et al., 2009). Sweeps occur less frequently within canopies, but have a greater contribution to momentum exchange than ejections, suggesting that sweeps are a primary contributor to downward momentum exchange resulting from fast moving downward gusts that penetrate the canopy (Lee and Black, 1993; Yue et al., 2007).

This paper presents novel results from high-frequency measurements of three-dimensional turbulent velocity at several locations over a vegetated foredune during

storm wind conditions. The purpose of the study was to quantify and examine patterns in, and properties of, airflow behaviour and decomposed turbulent Reynolds stress signals that drive surface stress generation with the goal of improving understanding of the aeolian sand transport process over foredunes. From this, interactions between turbulent flow, topographic forcing effects (e.g., streamline curvature and compression) and dune position are explored and implications for dune morphodynamics are discussed.

2.3. Study Site

The study site is located on a stretch of foredune within the Greenwich Dunes in Prince Edward Island National Park, Canada (Figure 2.2). This site has been the focus of previous research on beach-dune airflow and sand transport dynamics (e.g., Hesp et al., 2005; Walker et al., 2006; Davidson-Arnott et al., 2008; Bauer et al., 2009; Bauer et al., 2009; Davidson-Arnott et al., 2009; Davidson-Arnott and Bauer, 2009; Hesp et al., 2009; Walker et al., 2009a; Walker et al., 2009b; Delgado-Fernandez and Davidson- Arnott, 2011). The foredune extends to approximately 8.5 m above mean sea level, has a stoss slope (windward slope) steepness of 15° to 23°, and a crestline oriented approximately ENE (76°to 256°). At the time of the study, the toe of the foredune had a 0.6 m scarp formed by a preceding high-water event that removed the incipient foredune. The beach fronting the foredune is micro-tidal (~1 m) and had a low tide width of approximately 35 m. The beach is composed predominately of quartz sand with an average diameter of 0.26 mm. The dune was vegetated by American beach grass (*Ammophlia breviligulata*) and at the time of the experiment (October), near the end of the growing season, plant heights

ranged from 0.2 m to 0.6 m and densities were 40% to 70%. During the winter months this dune system is covered in snow and fronted by shorefast ice.

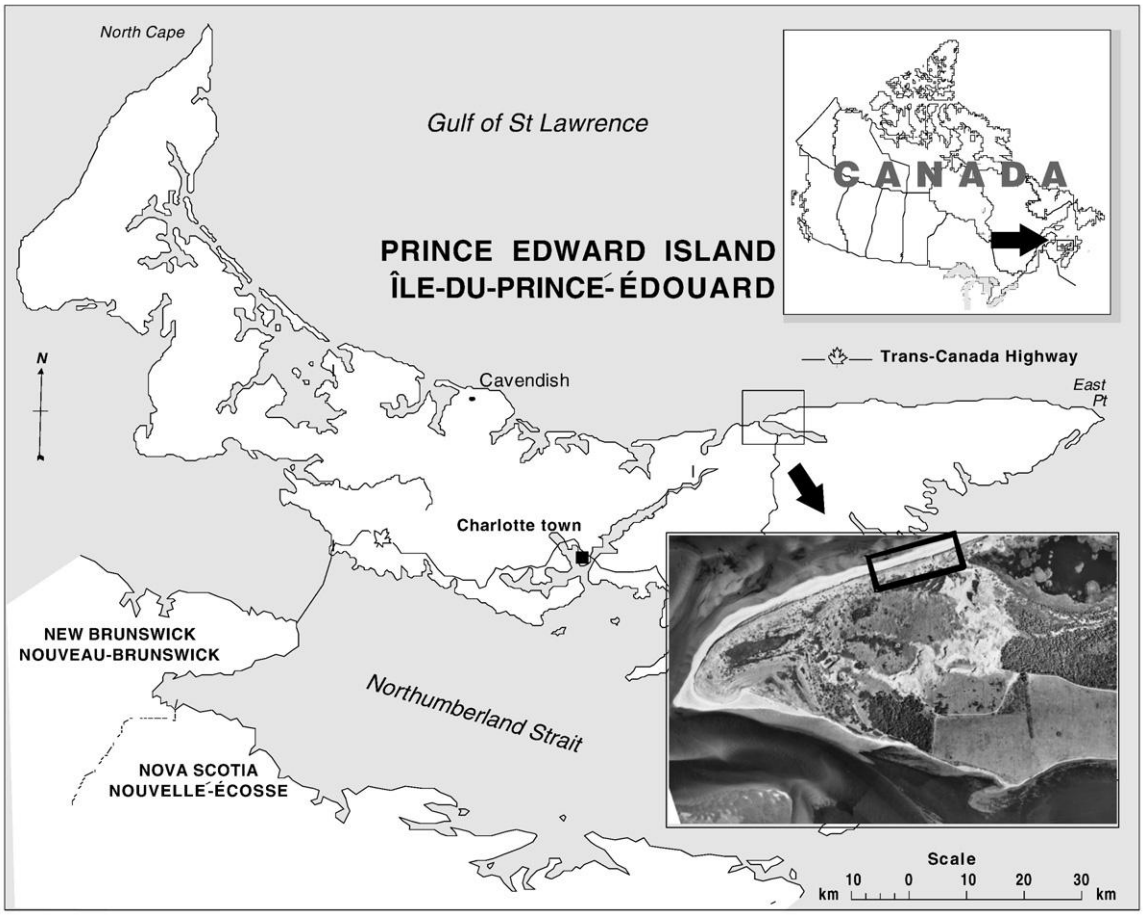

Figure 2.2: Location of study area.

Environment Canada meteorological data for 1995 to 2000 from Stanhope (~25 km to the southwest on the coast) show that prevailing summer winds in this area are from the southwest (obliquely offshore). Although these winds are frequent, they are often not competent to transport sediment. Instead, strong onshore winds from the north through northwest in the fall and winter are more favourable for onshore transport and dune maintenance (Pearce and Walker, 2005; Hesp et al., 2005; Walker et al., 2006). Delgado-Fernandez and Davidson-Arnott (2010) found that a large portion of the total sediment flux over a 9 month period was moved by a few small to medium (8- 12 m s^{-1}) wind events and that the angle and fetch are more important than strong winds. Strong wind events saw wave scarping and foredune erosion instead of large amounts of sand transport (Delgado-Fernandez and Davidson-Arnott, 2010). During the winter months, which is the windiest season, was the least important for sand transport due to a frozen beach and snow/ice cover (Delgado-Fernandez and Davidson-Arnott, 2010).

The wind event examined in this study occurred on 11 October 2004 between 0900 h and 1800 h AST during the approach of Tropical Storm "Nicole" in the Gulf of St. Lawrence region (see also Bauer et al., 2009; Davidson-Arnott and Bauer, 2009; Hesp et al., 2009; Walker et al., 2009a; Walker et al., 2009b). Hourly regional wind and climate conditions were measured at 5 m on a nearby meteorological station several hundred metres behind the foredune. Wind speeds increased from 14 to 28 m s^{-1} between 0900 h and 1700 h and were accompanied by light rainfall (0.60 mm total) from 1400 h to 1700 h and the wind direction was obliquely onshore (ENE) (Figure 2.3). Incident wind conditions on the beach measured at 4 m showed speeds ranging from 6 m s^{-1} to > 20 m s^{-1} between 0900 h and 1700 h (Figure 2.3). Wind direction was alongshore to

obliquely onshore and sediment transport developed on the beach after 1100 h as the wind speed approached and exceeded 20 m s^{-1}. Detailed velocity profile responses over this same dune profile during this storm event are described in Hesp et al. (2009).

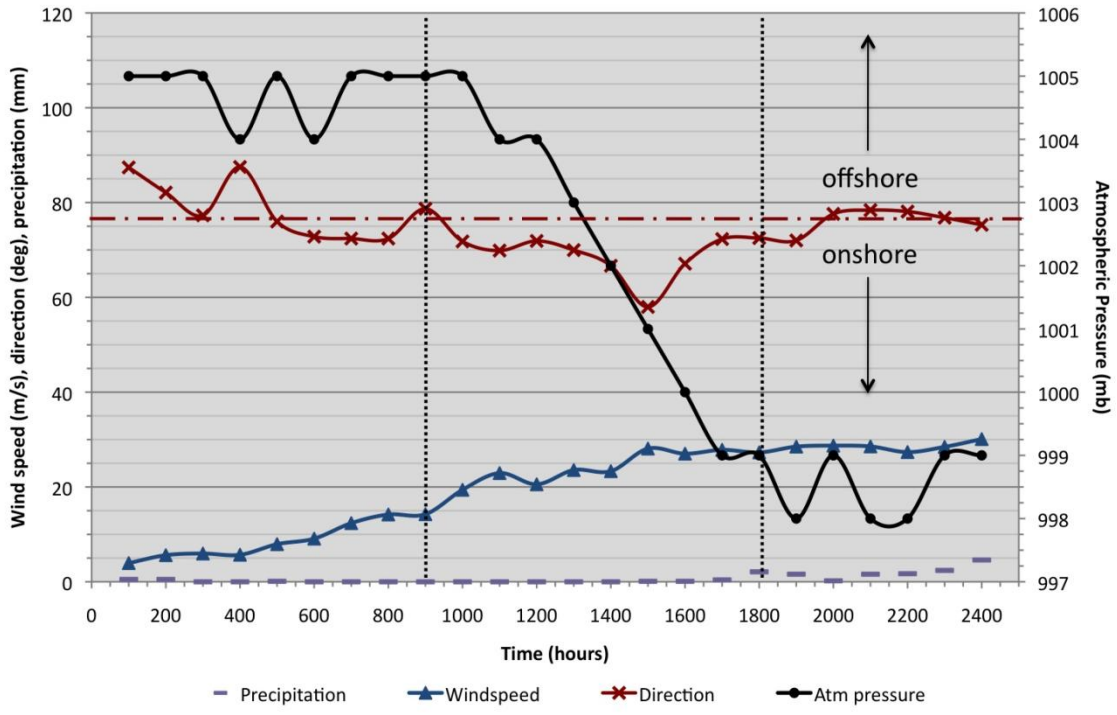

Figure 2.3: Meteorological conditions for 11 October 2004 showing precipitation, wind speed, directions, and atmospheric pressure.

2.4. Methods

2.4.1. Instrument Deployment

Three-dimensional velocity components, (u, oriented alongshore; v, oriented off-onshore; w, vertical) were measured using RM Young 81000 sonic anemometers at four different locations (toe, stoss, crest, lee) along a shore-normal transect over the dune (Figure 2.4). At some locations, instruments were deployed at two different heights (near-surface stations at 0.6 m and upper stations at 1.66 m). Station 1, located at the toe of the dune, measured incident outer flow conditions at 2.05 m. Stations 2 and 3 were located at the mid-point of the stoss slope at 0.60 m and 1.66 m and stations 4 and 5 were located at the crest at 0.60 m and 1.66 m, respectively. Station 6 was located in the lee at 0.60 m. Instruments as deployed are shown in Figure 2.5. All instruments were sampled at 32 Hz by a Campbell Scientific CRX10 data logger and a notebook computer. Instruments were oriented relative to true north and u-v axial planes were aligned to the underlying surface slope in order to avoid streamline misalignment to the sensor sampling plane (Walker, 2005). U-axes of instruments were oriented into the dominant (alongshore) flow direction and V-axes were oriented spanwise to the dominant flow (i.e., on-off shore). Flow visualization using flow streamers was used to verify the alignment. Pitch and yaw rotation was also applied to the data to correct for any remnant streamline misalignment effects as described below.

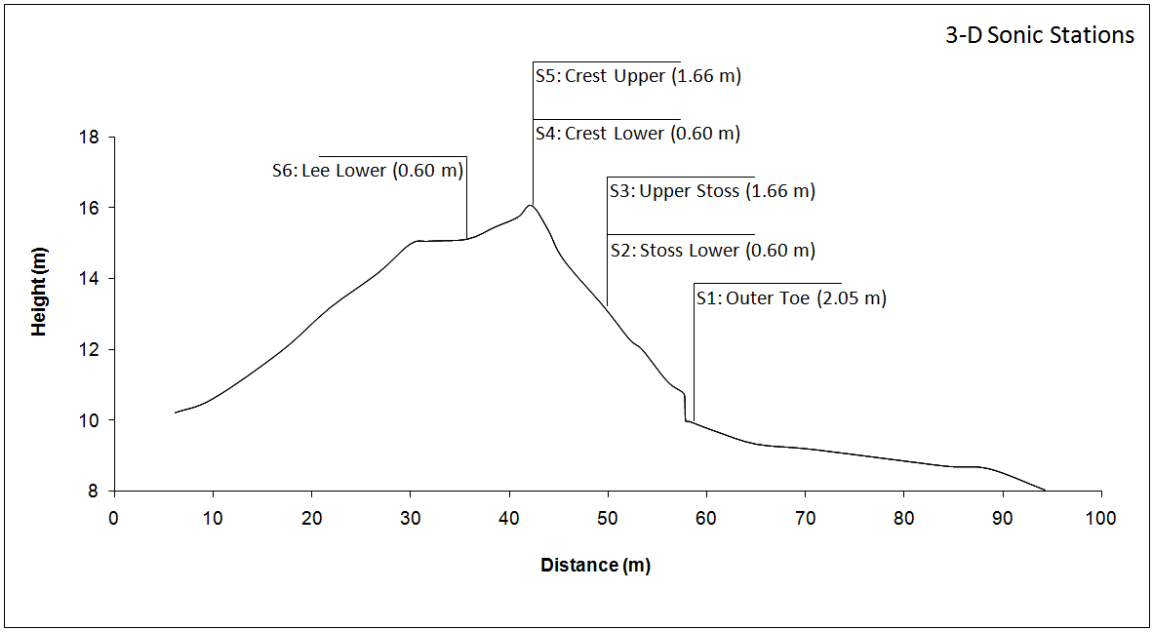

Figure 2.4: Profile of the dune system showing the location of the six different stations.

(a)

(b)

Figure 2.5: Photographs of the study site. (a) The transect ran from the toe of the dune to the crest and had a total of four different locations with six stations. (b) The stations were located at two different heights, 1.66 m and 0.60 m, and were aligned with the underlying surface slope.

2.4.2. Data Description and Analyses

Data explored in this paper are derived from a population of 12 ten-minute runs, recorded between 1035 and 1720 h on 11 October 2004. At a sampling frequency of 32 Hz, each run contained a maximum of 19200 observations. A subset of four runs (Runs 1, 4, 7, and 10) were chosen for detailed analyses based on minimal missing data (i.e., less than 1%) and to capture a range of incident flow angles and resultant speeds (Table 2.1). General flow conditions from the larger population of runs spanned 30 to 47° incident flow direction (where 0° = alongshore, 90° = onshore, -90° = offshore) and 9 to 14 m s^{-1} as measured at the upper crest location.

Observed velocity data (u_x, v_z, w_y) were rotated for yaw and pitch to correct for possible sensor misalignment to local streamlines (Roy et al., 1996; van Boxel et al., 2004; Walker, 2005). Yaw correction used the following equations:

$$u_1 = u_x \cos\alpha + v_z \sin\alpha \tag{2.5}$$

$$v_1 = -u_x \sin\alpha + v_z \cos\alpha \tag{2.6}$$

$$\alpha = \arctan\left(\frac{V_z}{U_x}\right) \tag{2.7}$$

where u_1 and v_1 are yaw corrected values, alpha (α) is the time averaged angle for flow, and U and V indicate time averaged values. This correction adjusts the u component toward the mean flow vector and forces the mean v component to zero. Pitch rotation used the following equations:

$$u_2 = u_x \cos\varphi + w_y \sin\varphi \tag{2.8}$$

$$w_2 = -u_x \sin\varphi + w_y \cos\varphi \tag{2.9}$$

$$\varphi = \arctan\left(\frac{W_y}{U_x}\right) \tag{2.10}$$

where u_2 and w_2 are pitch rotated values from equations 2.5-2.7, phi (φ) is the angle of the incoming streamline relative to the sensor plane (which was mounted parallel to the dune surface), and U and W indicate time averaged values (Walker, 2005) (Table 2.1). This rotation forces the mean w component to zero, which implies that the u component is oriented exactly parallel to the streamlines. Quasi-instantaneous prime values were then derived using pitch rotated values in equations 2.1 and 2.2 and, from this, kinematic Reynolds stress (RS_k) values were calculated using equation 2.4 (Table 2.1).

Summary statistics (Table 2.1) were calculated including u, v, and w time-averages (U, V, W), standard deviations (σ), minima, maxima, resultant (UV) vector magnitude, and streamwise and vertical flow steadiness, using a coefficient of variation ($CV_{u\ or\ w}$) as follows:

$$CV_u = \frac{\sigma_u}{U} \tag{2.11}$$

Turbulence intensity, characterised using total kinetic energy (TKE), was calculated using:

$$TKE = \frac{1}{2}[(\sigma_u{}^2) + (\sigma_v{}^2) + (\sigma_w{}^2)] \tag{2.12}$$

Reynolds stress decomposition was performed on the rotated velocity datasets for u and w to produce quadrant plots and corresponding activity frequency counts at each location for runs 1, 4, 7, and 10. Resulting quadrant plots provide a visual representation of the frequency distribution of activities that dominate the flow signal. To aid interpretation of the distributions, quadrant plots were produced using all observations and percentage quartile isopleths (i.e., 25%, 50%, 75%, and 100% of observations) including a 1% observation (represented by an X) that indicates the central point of the data distribution. Quadrant activity frequencies (Table 2.2), however, were derived from

only significant stress activities that exceed a threshold (H) value of one standard deviation of RS_k, as is commonly recommended (Lu and Wilmarth, 1973).

Flow exuberance, EX_{FL}, describes the shape of the quadrant frequency distribution using the ratio of total Q1 and Q3 interaction activities to Q2 and Q4 activities (Shaw et al., 1983; Yue et al., 2007):

$$Exuberance_{Flow}(EX_{FL}) = \frac{Quadrant\ 1 + Quadrant\ 3}{Quadrant\ 2 + Quadrant\ 4} \quad (2.13)$$

In effect, exuberance expresses the ratio of the negative to positive contributions to RS generation. When the ratio is close to one, there is an even distribution of activities occurring in all four quadrants (i.e., a circular quadrant plot), whereas exuberance values approaching zero indicate the dominance of Q2 ejections and Q4 sweeps (i.e., a skewed elliptical quadrant plot as expected for strongly sheared flows).

2.5. Results

2.5.1. Flow Dynamics and Responses to Changes in Incident Flow Angle

Mean and turbulent flow properties over foredunes are sensitive to changes in incident flow angle and are controlled by topographic forcing and steering (e.g., Walker et al. 2009a; 2009b; Lynch et al., 2009). Average flow conditions and turbulent flow properties for the subset of four runs are shown in Table 2.1. Figures 2.6 through 2.8 show how normalized resultant wind speed ($UV/UV_{crest\ upper}$), kinematic Reynolds stress (RS_k), and flow exuberance (EX_{FL}) respond to changing incident wind speed and/or flow direction over the foredune. During the measurement period, incident flow angles in outer flow at the dune toe (crest lower) were alongshore to obliquely onshore and averaged

from 21 to 31° (41 to 53°). Notable alongshore topographic steering occurred toward the crest of the dune during these runs by as much as 13° at upper flow stations and 22° in near-surface flow at the vegetation canopy for run 7 (e.g., from 31° incident at the dune toe to 44° for crest upper flow and 53° for crest near-surface flow). These observations support the findings of Walker et al. (2009 b) who documented similar deflection ranges on a nearby segment of foredune during the same wind event. Lee-side flow was separated and reversed for all runs and ranged in direction (speed) from -5° (-3.23 m s^{-1}) during run 1 to -28° (-2.30 m s^{-1}) during run 7.

Table 2.1: Summary of the flow properties: incident flow angle (IFA) (degrees), resultant speed (m s^{-1}), total kinetic energy (TKE) (m^2s^{-2}), Reynolds stress (RS) (u'w'), and flow exuberance ((Q1+Q3)/(Q2+Q4)). Observed values were used for U, V, and W, resultant speed, and TKE whereas, rotated values were used for the RS and IFA.

	Toe (2.05 m) (-11°)	Stoss Lower (0.60 m) (-19°)	Stoss Outer (1.66m) (-19°)	Crest Lower (0.60 m) (-23°)	Crest Outer (1.66 m) (-23°)	Lee Outer (0.60 m) (+7°)
Run 1 (10:29-10:39)						
Flow Angle (°)	22	29	27	43	32	-5
U [CV_u]	7.03 [0.15]	3.41 [0.39]	6.38 [0.22]	4.63 [0.29]	7.48 [0.16]	3.22 [0.31]
V	2.84	1.92	3.20	4.32	4.70	-0.25
UV	7.58	3.91	7.13	6.33	8.83	3.23
W [CV_w]	1.22 [0.34]	-0.10 [-6.90]	-0.06 [-11.63]	-0.39 [-1.65]	-0.96 [-0.58]	0.42 [1.71]
Streamline angle (°)	-2	-18	-19	-18	-16	14
TKE	0.84	1.74	1.80	1.79	1.26	1.16
RS	0.22	0.40	0.47	0.28	0.14	0.06
Run 4 (12:39- 12:49)						
Flow Angle (°)	21	28	26	41	31	-21
U [CV_u]	7.95 [0.14]	4.27 [0.36]	7.47 [0.21]	5.46 [0.28]	8.49 [0.16]	2.11 [0.43]
V	3.10	2.28	3.58	4.80	5.10	-0.82
UV	8.53	4.84	8.29	7.27	9.90	2.26
W [CV_w]	1.36 [0.36]	-0.10 [-7.83]	-0.06 [-14.20]	-0.45 [-1.60]	-1.00 [-0.63]	0.33 [2.13]
Streamline angle (°)	-2	-18	-19	-18	-16	16
TKE	1.18	2.31	2.46	2.42	1.79	1.10
RS	0.23	0.44	0.59	0.34	0.19	-0.02
Run 7 (14:42- 14:52)						
Flow Angle (°)	31	42	37	53	44	-28
U [CV_u]	8.20 [0.16]	4.88 [0.34]	8.70 [0.16]	6.31 [0.28]	9.04 [0.17]	2.03 [0.55]
V	4.94	4.44	6.53	8.31	8.62	-1.08
UV	9.57	6.60	10.88	10.43	12.49	2.30
W [CV_w]	1.90 [0.30]	-0.45 [-2.28]	-0.23 [-2.70]	-0.83 [-0.91]	-1.55 [-0.46]	-0.01 [-106.3]
Streamline angle (°)	2	-14	-18	-16	-13	7
TKE	1.48	3.27	2.00	2.82	2.11	2.14
RS	0.38	0.76	0.30	0.24	0.12	-0.14
Run 10 (16:49- 16:59)						
Flow Angle (°)	28	37	32	49	39	-23
U [CV_u]	9.47 [0.18]	5.82 [0.32]	10.28 [0.17]	7.68 [0.25]	10.94 [0.16]	2.49 [0.49]
V	5.12	4.47	6.52	8.84	9.01	-1.08
UV	10.76	7.34	12.17	11.71	14.17	2.71
W [CV_w]	2.02 [0.43]	-0.30 [-3.69]	-0.14 [-5.72]	-0.88 [-0.89]	-1.54 [-0.49]	-0.01 [104.5]
Streamline angle (°)	1	-16	-18	-17	-15	7
TKE	2.81	4.11	3.17	3.44	2.71	2.73
RS	0.53	0.96	0.53	0.28	0.18	-0.26

Resultant (UV) incident wind speeds in outer flow at the dune toe (at 2.05m) increased throughout the day as tropical storm "Nicole" approached, ranging from 7.58 (run 1) to 10.76 m s^{-1} (run 10). On the stoss slope, near-surface speeds increased from the lower stoss to the crest by approximately 3 to 4 m s^{-1}, which translates to a flow speedup of about 33 to 38% due to streamline compression. Resultant speeds were slowest in the lee separation zone, ranging from 2.26 (run 4) to 3.23 (run 1) m s^{-1} or approximately 24 to 42% of incident flow measured at the dune toe (a 58 to76% reduction). The crest location was most responsive to changes in incident flow angle, due to maximum streamline compression effects (Hesp et al., 2005).

Figure 2.6 shows that normalized resultant wind speeds ($UV/UV_{crest\ upper}$) increased with more onshore flow directions on the upper dune slope. Relations were most responsive (i.e., steepest slope) and very strong (R^2=0.86) at the crest lower station where streamline compression and flow acceleration are pronounced. Distinct flow deceleration (i.e., strong, negative relation) occurred with more onshore flow angles at the toe station as expected due to flow stagnation in this region. Near-surface flow in the lee showed a relatively weak (R^2=0.31) negative relation between resultant windspeed and incident flow angle with more onshore flow, due to increased sheltering and flow separation development.

Streamwise flow steadiness values (CV_u, Table 2.1) are large (unsteady) at the near-surface stoss location and in the lee, and small (steady) in outer flow at the toe and crest locations. Lee values are negative owing to reversed flow (-u). Vertical flow steadiness (CV_w) also shows similar spatial patterns across runs with greatest unsteadiness in upper flow on the stoss and in near-surface flow in the lee.

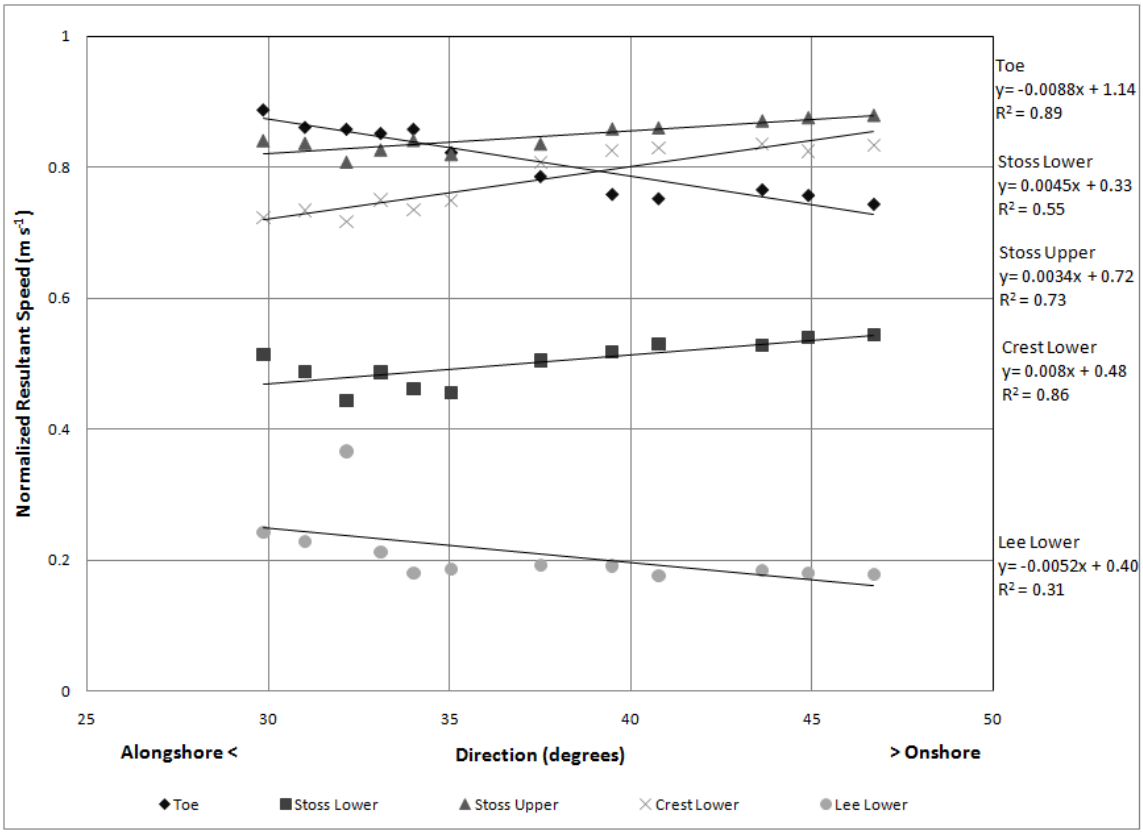

Figure 2.6: Response of time-averaged resultant speed (m s^{-1}) normalized to the upper crest to changing incident flow angles for 12 10-minute runs between 0900 h and 1800h.

Reynolds stress values were typically lower in flow at the dune toe, a minimum in the lee, and highest at the stoss slope stations (upper stoss for runs 1 and 4, near-surface stoss for runs 7 and 10). In the lee, RS_k values increased with incident wind speed and approached those for upper flow at the crest for run 10. Generally, RS_k values increased at all locations as incident wind speed increased and incident flow direction increased (i.e., became more onshore).

Reynolds stress showed moderately strong relations ($R^2 > 0.6$) with increasing (more onshore) incident wind direction at the toe, stoss, and lower crest locations and very strong ($R^2 > 0.9$) relations with incident wind speed at the lower stoss and toe locations (Figure 2.7). The most sensitive (i.e., steepest slope) relations with both wind speed and direction occurred at the lower stoss location while response sensitivities were slight (low slopes) at both crest stations. Generally, as flow became more onshore, or faster, RS_k increased at the toe and lower stoss slope locations (+ve slope relations) while RS_k decreased during more onshore flow, or slower speeds (-ve slope relations) at upper stoss, crest, and lee locations. Thus, over the population of runs presented here, there is a defined spatial pattern and topographically controlled shift in RS dynamics from the lower to upper dune slope.

(a)

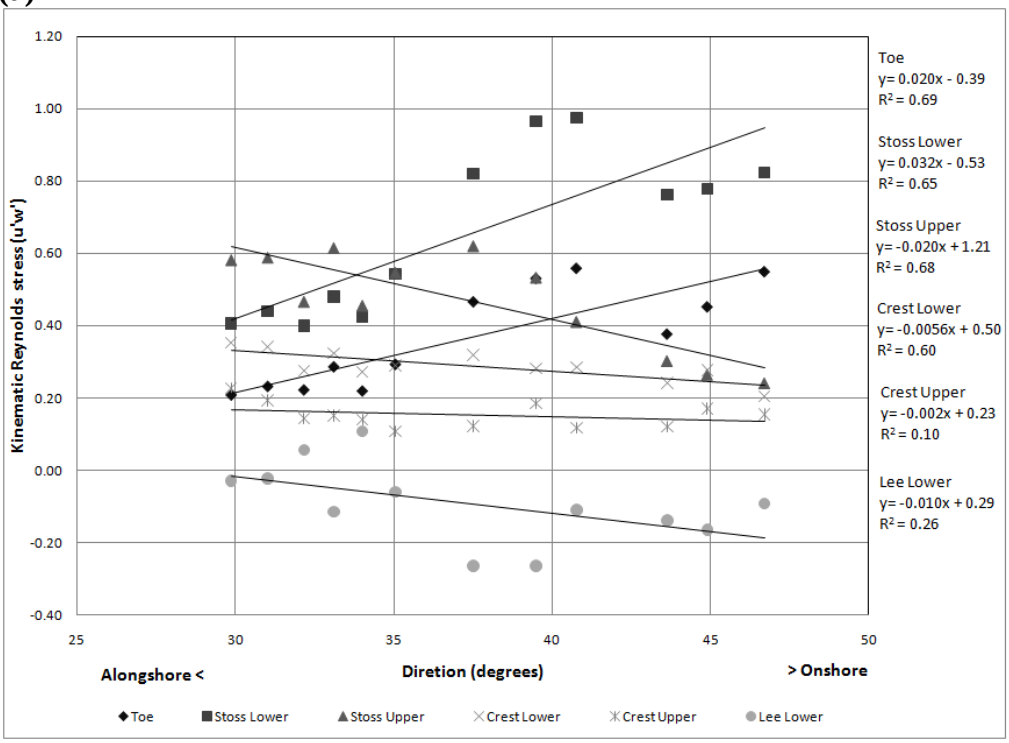

(b)

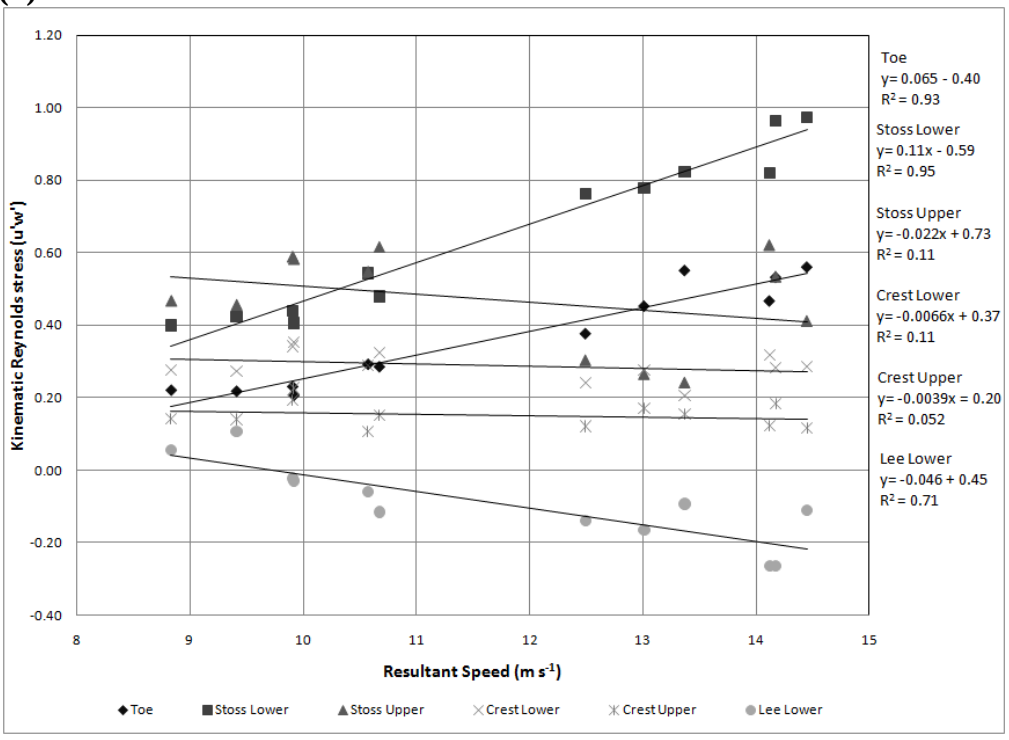

Figure 2.7: (a) Response of time-averaged Reynolds stress (RS)(u'w') to changing incident flow angles for 12 10-minute runs between 0900 h and 1800 h. (b) Response of time averaged Reynolds stress (RS) (u'w') to changing resultant speeds (m s^{-1}) for 12 10-minute runs between 0900 h and 1800 h.

Flow exuberance showed strong ($R^2 > 0.7$) relations with more onshore (increasing) incident flow direction at the upper stoss and crest locations as well as with increasing wind speed at both crest locations (Figure 2.8). The most sensitive relations (i.e., steepest slopes) with both wind speed and direction occur in the lee, then both crest locations and at the upper stoss location. As with RS_k, there is an interesting (though inverse) spatial pattern in flow exuberance response over the dune; as flow became more onshore, or faster, EX_{FL} values increase at the upper stoss, crest, and lee locations (+ve slope relations) yet decrease during more onshore flow, or slower speed conditions (-ve slope relations) at the toe and lower stoss slope locations. This indicates a spatial pattern in the prevalence of Q2 ejection and Q4 sweep activities (that contribute positively to RS generation) over Q1 and Q3 interactions (that contribute negatively to RS) over the dune. Generally, Q2 ejection and Q4 sweep activities occurred more frequently on the lower stoss slope and dune toe locations, while flow at the upper stoss and both crest locations experience increasingly frequent (though not dominant) contributions from Q1 and Q3 interactions. Furthermore, as flow direction shifts onshore and/or wind speed increased, the frequency of Q1 and Q3 activities increased at these upper dune locations and in the lee. This ‘exuberance effect’ may result from changing flow dynamics and turbulence generation associated with topographically forced streamline curvature and compression effects (cf. Wiggs et al. 1996) that alter the spatial distribution of Reynolds stress and contributing quadrant ‘activities’ over the dune.

(a)

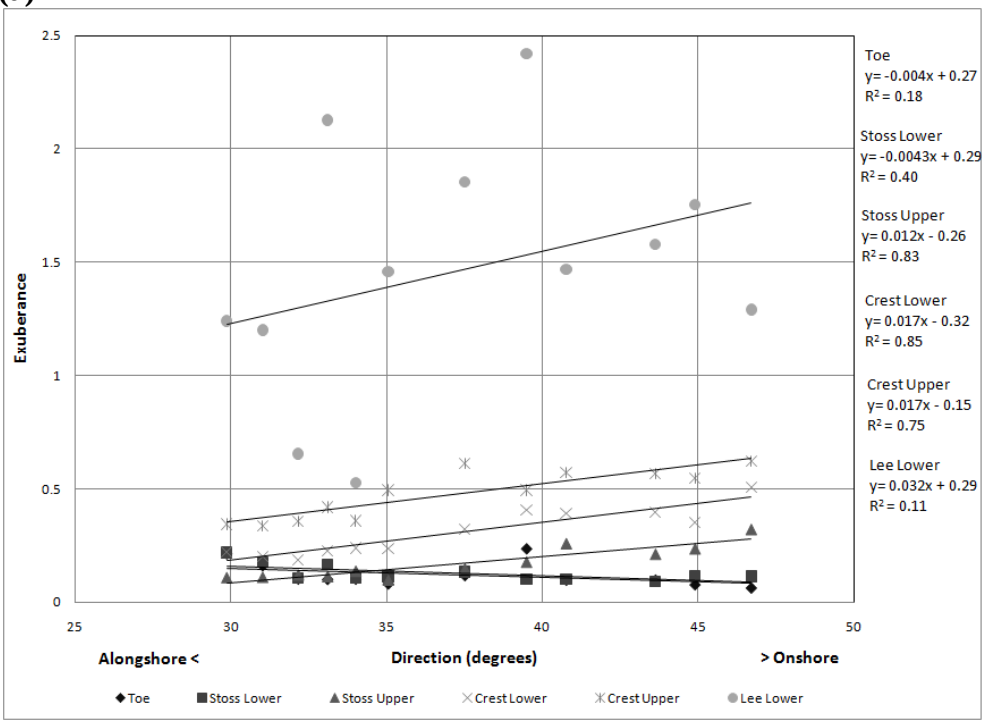

(b)

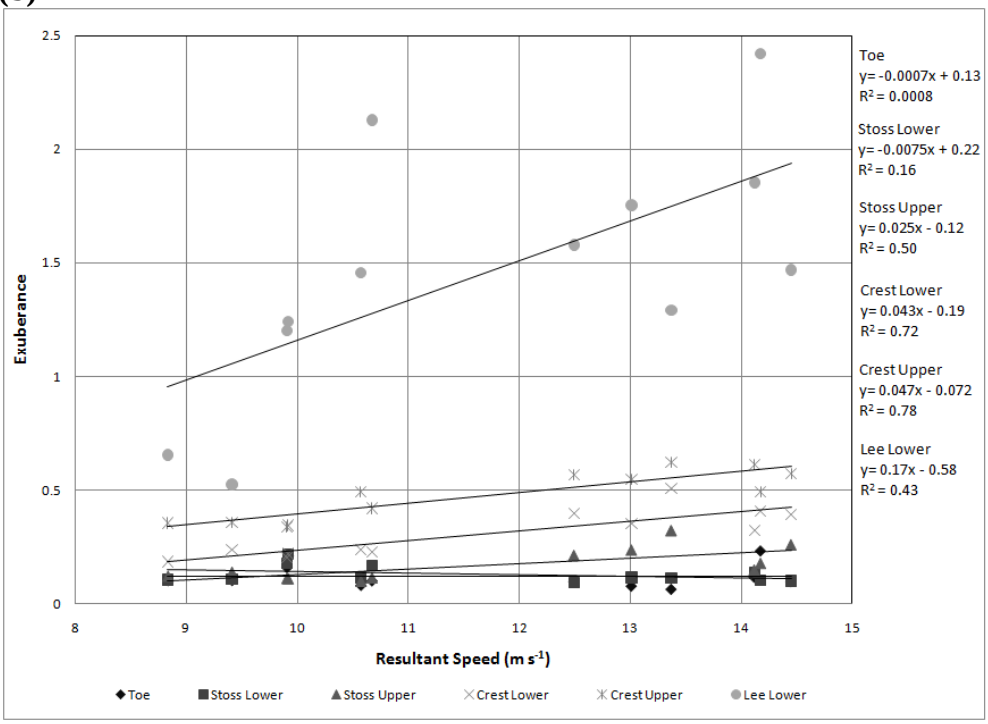

Figure 2.8: (a) Response of time-averaged flow exuberance ((Q1+Q3)/(Q2+Q4)) to changing incident flow angles for 12 10-minute runs between 0900 h and 1800 h. (b) Response of time-averaged exuberance ((Q1+Q3)/(Q2+Q4)) to changing resultant speeds (m s^{-1}) for 12 10-minute runs between 0900 h and 1800 h. The values used to calculate flow exuberance were the significant values for each quadrant (1 standard deviation).

2.5.2. Quadrant Analysis

Significant quadrant activities were derived by removing activities from below 1 standard deviation of the dataset. These values are shown in Table 2.2, along with corresponding flow exuberance values and Q2:Q4 ratios, and describe activity distributions shown in Figures 2.9 and 2.10 for runs 1 and 10 respectively. Essentially, these values, each specific quadrant count and the exuberance values, confirm and highlight the 'exuberance effect' identified above. It must be noted that the prime values used to construct Figures 2.9 and 2.10 are not the up and down values of u and w. The up and down values for u and w are shown in Table 2.1 as 10 minute averages of U and W.

Table 2.2: Summary of the significant quadrant activity counts (1 standard deviation removed), quadrant 2 to quadrant 4 ratio (Q2/Q4), and exuberance ((Q1+Q3)/(Q2+Q4)).

	Toe (2.05 m)	Stoss Lower (0.60 m)	Stoss Outer (1.66 m)	Crest Lower (0.60 m)	Crest Outer (1.66 m)	Lee (0.60 m)
Run1 (10:29-10:39)						
Quad 1	140	163	100	170	271	362
Quad 2	1159	1091	1295	1025	944	694
Quad 3	87	66	152	156	278	424
Quad 4	1072	1100	797	733	603	508
Q2:Q4	1.08	0.99	1.62	1.40	1.57	1.37
Exuberance	0.10	0.10	0.12	0.19	0.35	0.65
Run 4 (12:39- 12:49)						
Quad 1	184	260	76	153	215	377
Quad 2	1015	959	1292	983	913	473
Quad 3	132	68	148	186	283	672
Quad 4	965	902	737	704	569	401
Q2:Q4	1.05	1.06	1.75	1.40	1.60	1.18
Exuberance	0.16	0.18	0.11	0.20	0.34	1.20
Run 7 (14:42- 14:52)						
Quad 1	123	101	178	249	344	473
Quad 2	1025	1125	919	851	807	408
Quad 3	81	92	167	276	343	721
Quad 4	1069	995	706	471	407	348
Q2:Q4	0.96	1.13	1.30	1.81	1.98	1.17
Exuberance	0.10	0.09	0.21	0.40	0.57	1.58
Run 10 (16:49- 16:59)						
Quad 1	114	133	139	238	384	649
Quad 2	855	1054	1058	847	753	319
Quad 3	267	85	159	306	283	738
Quad 4	774	1079	622	487	598	254
Q2:Q4	1.10	0.98	1.70	1.74	1.26	1.26
Exuberance	0.23	0.10	0.18	0.41	0.49	2.42

Quadrant activity distributions changed with location on the dune and with variations in incident flow angle and speed (Figures 2.9 and 2.10). Early in the day (run 1, Figure 2.9) quadrant plots were more compact (i.e., there is less scatter), whereas during faster and slightly more onshore flow in run 10 (Figure 2.10), quadrant plots show greater scatter in both u' and w' axes (see also TKE values in Table 2.1). For all locations and runs (except in the lee for run 1), quadrant distributions showed a clear skewness in favour of ejection and sweep activities. Typically, exuberance is smallest at the toe and stoss (upper and lower) locations, which suggests that Q2 and Q4 activities dominate stress generation on the lower windward slope of the dune (Table 2.2). Significant ejections generally exceed sweeps at most locations, except on the lower stoss and dune toe locations, where they are similar in frequency, and in the lee (all runs) where sweeps dominate.

Outer flow incident to the dune toe during run 1 showed a relatively flat w' distribution and balanced frequencies of Q2 and Q4 activities reflecting more isotropic turbulence. During faster flow of run 10, the quadrant distribution showed significant scatter toward more Q1 and Q3 interaction activities, many of which are not significant (compare values shown in Figure 2.10 with Table 2.2). Total ejection and sweep activities remain similar between runs 1 and 10, however, the number of significant Q2 and Q4 activities drops during the faster run 10, while more significant Q1 and Q3 interactions occurred and exuberance values increased from 0.10 to 0.23. Thus, the frequency of significant ejection and sweep activities appears to decline in exchange for more significant interaction activities that contribute negatively to RS generation, as incident flow becomes faster and more onshore.

Flow exuberance values were typically low on the stoss slope. At the upper stoss station, there was a greater frequency of upward ejection activities compared to downward sweep activities by 1.3 to 1.8 times (Table 2.2). At the crest, quadrant distributions for upper flow were less skewed toward ejections and sweeps (i.e., higher exuberance values), whereas near-surface quadrant distributions were very similar in form and frequency to upper flow at the stoss location, with slightly higher exuberance.

In the lee, quadrant distributions for all runs were more symmetrical than on the windward slope indicating isotropic turbulence. This is demonstrated by comparatively high exuberance values resulting from a greater frequency of Q1 and Q3 interactions, which are typically most frequent in the lee, and a decline in Q2 ejection activity, which are the least frequent in the lee. This shift in quadrant distributions and activity frequencies reflects complex, separated, and often reversed flow that was present in the lee of the crest (Table 2.1).

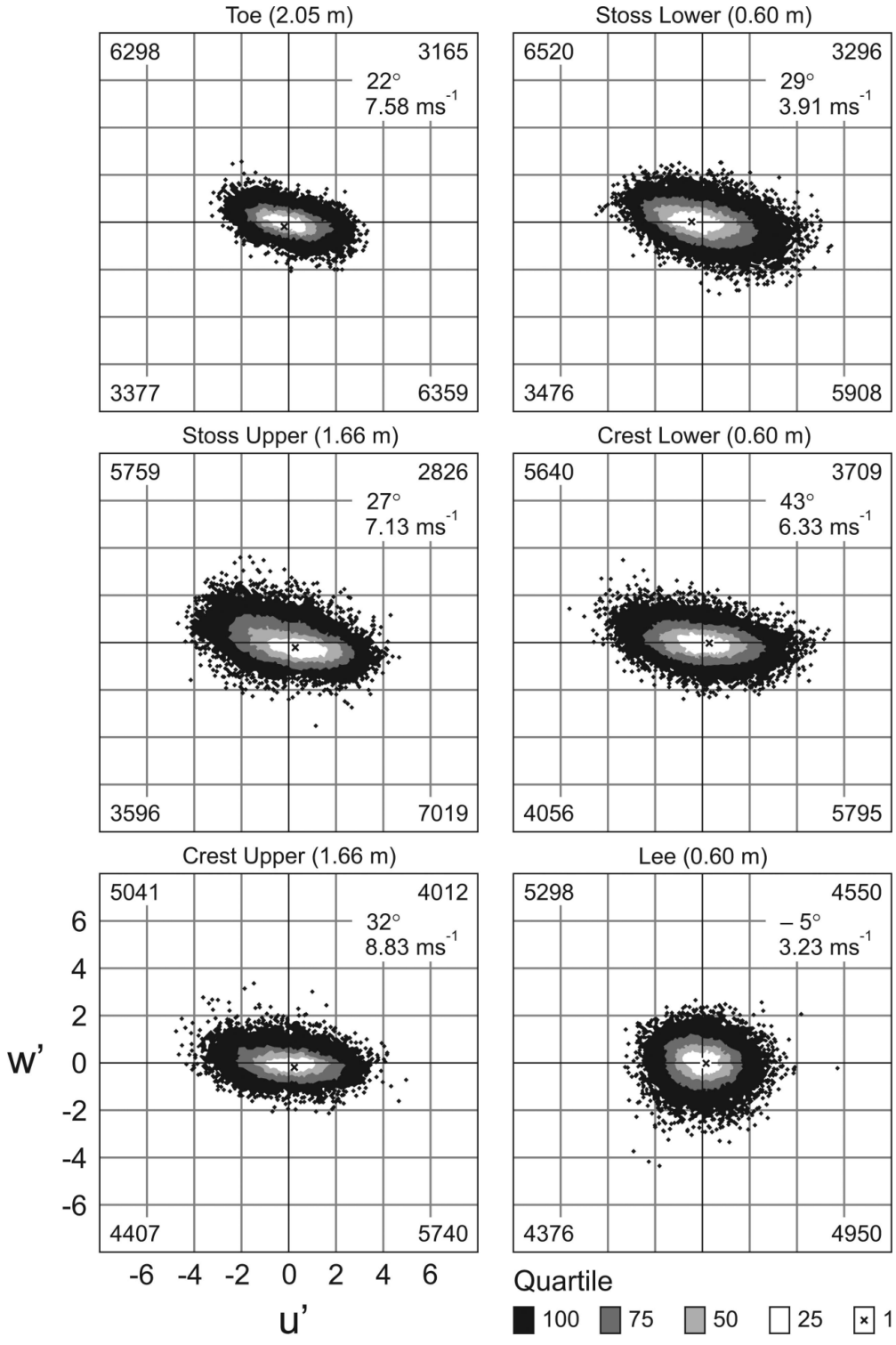

Figure 2.9: Run 1 quasi- instantaneous (32 Hz) quadrant plots for a 10 minute run (n= 19200) occurring at 0900 h on 11 October 2004 during the approach of tropical storm "Nicole". In the top right hand corner is the incident flow angle and the resultant speed. In each quadrant is a quadrant count that represents the total number of activities that occurred within.

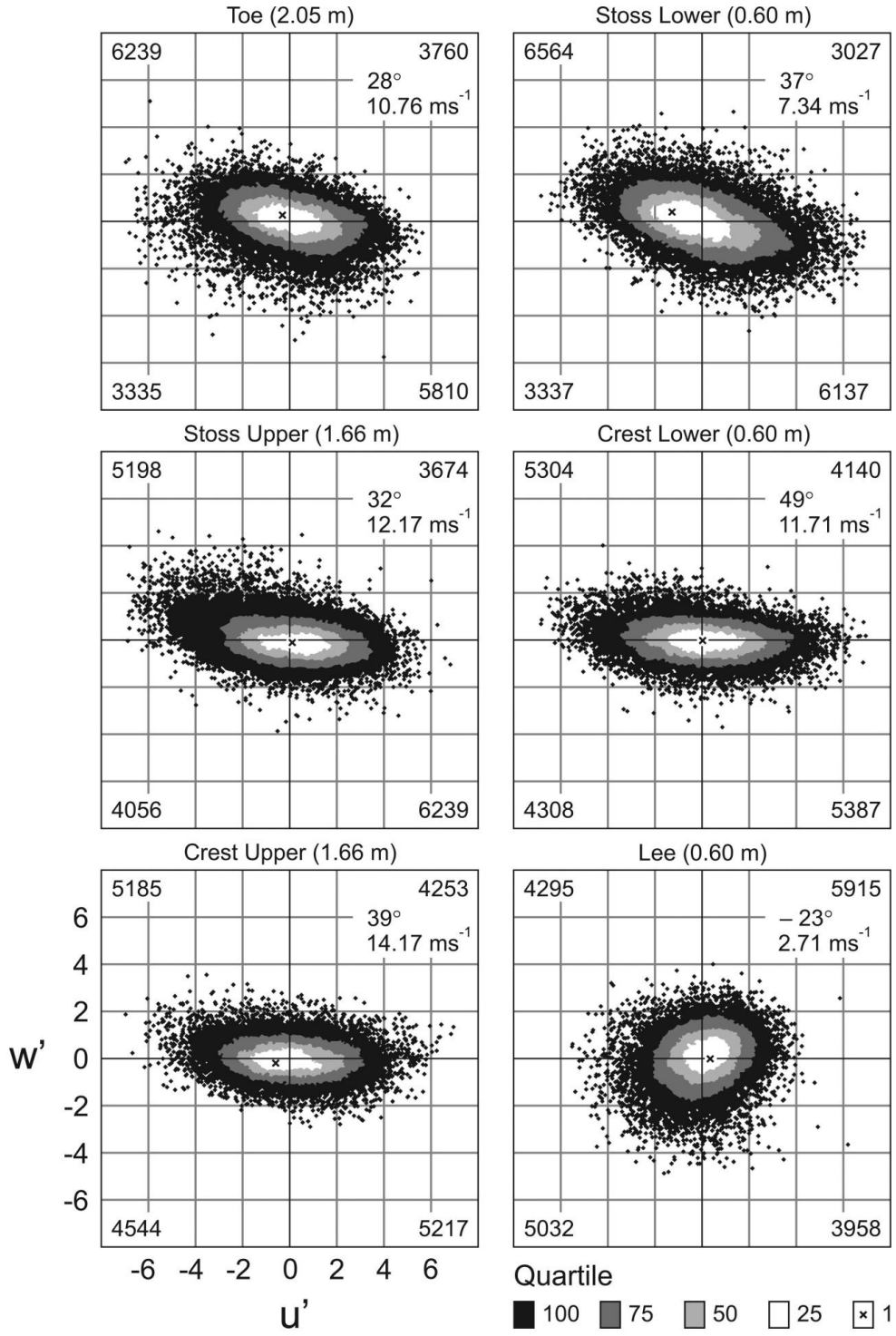

Figure 2.10: Run 10 quasi- instantaneous (32 Hz) quadrant plots for a 10 minute run (n= 19200) occurring at 1700 h on 11 October 2004 during the approach of tropical storm "Nicole". In the top right hand corner is the incident flow angle and the resultant speed. In each quadrant is a quadrant count that represents the total number of activities that occurred within.

2.6. Discussion

2.6.1. Effects of Topographic Forcing on Turbulent Reynolds Stress Generation

This paper is the first to demonstrate that the turbulent bursting process and related quadrant activity distributions are influenced by topographic forcing of airflow over coastal foredunes. Along the lower windward slope of the dune (toe, stoss locations) topographic forcing causes a decrease in flow exuberance and an increase RS_k whereas, at the crest, there is an increase in exuberance and a decrease in RS_k. The comparison of streamline angles to underlying surface angles (Table 2.1) shows that concave streamline curvature exists at the foredune toe, streamlines are essentially parallel to the surface on the stoss, and curvature is convex at the crest. Observed differences in turbulent flow properties and Reynolds stress generation arise from these topographic forcing effects. For instance, concave streamline curvature at the toe of a dune tends to destabilize flow and result in increased shear stress generation via conveyance of turbulent structures towards the surface (Wiggs et al. 1996; Walker and Nickling, 2002; 2003).

Near-surface Reynolds stresses were highest in near-parallel flow at either the upper or near-surface stoss locations with maximum RS_k values more than double (1.8 to 2.6 times) that for incident outer flow at the foredune toe. Areas of high Reynolds stresses demonstrated a higher frequency of Q2 ejection and Q4 sweep activities, which are thought to play a role in initiating sand transport. In the lee, RS_k values were lowest and the frequency of Q1 and Q3 interactions that contribute negatively to RS generation were highest. Reynolds stress values at all near-surface locations increased with faster incident wind speeds and more onshore flow angles and, correspondingly, Q2 and Q4 activity frequencies became more prevalent in upper flow at 1.66 m. The occurrence of

ejection and sweep activities generally decline toward the crest. It must be noted that the near-surface measurements were taken at 0.6 m above the surface, above the vegetation canopy, to avoid vegetation interaction effects. The height difference between the surface and anemometer thus limits the ability to interpret implications for sediment transport, due to the fact that the sonic anemometer may be recording a different eddy event (van Boxel et al. 2004).

Flow acceleration persists toward the crest, as evidenced by low-level, high-speed 'jets' around 1 m above the bed (see Hesp et al. 2009), RS_k values decrease up the stoss and into the lee. This is corroborated by a shift toward higher flow exuberance values, which suggest increasing frequencies of Q1 and Q3 interactions that contribute negatively to RS generation. Generally, RS_k values at the lower stoss location are greater than at the crest lower location (by 1.3 to 3.4 times) and the difference increases as incident winds become faster (Table 2.1). This demonstrates an 'exuberance effect' in near-surface airflow over dunes that results in an increase in activities that contribute negatively to Reynolds stress generation (Q1 and Q3) toward the crest (Table 2.2).

2.6.2. Implications for Sediment Transport and Dune Morphodynamics

Although sediment transport was observed but not measured in this experiment, the measured turbulent airflow behaviour and near-surface Reynolds stress patterns provide some basis for discussion of observed sediment transport and dune morphodynamics implications (Ollerhead et al., 2003; Ollerhead et al., 2005; Davidson-Arnott., 2007). Sand transport was observed moving in saltation and in modified suspension, during modified suspension sand can be transported hundreds of meters

allowing for it to be transport up and over the foredune and deposited in the lee and back dune (Arens, 1996; Anderson and Walker, 2006). In the fluvial literature, Q2 ejections and Q4 sweep activities have been linked to saltation and suspended sediment entrainment and transport (Jackson, 1976; Drake et al., 1988; Best, 1993; Robert et al., 1996; Best and Kostaschuk, 2002; Kostaschuk et al., 2008; Kostaschuk et al., 2009; Shugar et al., 2010). Here, Q2 ejection and Q4 sweep activities that contribute positively to RS generation had the greatest frequency in near-surface flow over the foredune and generally declined in frequency toward the crest. This decline in ejection and sweep activities that have been identified as important for sediment entrainment, coupled with a coincident drop in time-averaged RS_k toward the crest, suggests decreased sand transport potential and, thus, increased tendency for deposition toward the crest. Though speculative, this observation highlights a key knowledge gap regarding RS generation and sand transport over dunes. There is a paucity of data on contemporaneous relations between high-frequency turbulent Reynolds stress signals (and decomposed quadrant activities) and quasi-instantaneous sand transport, particularly as it relates to defining threshold conditions for grain entrainment and deposition. As such, it is difficult to ascribe RS values, activities, or trends to observed or predicted sediment flux patterns over flat surfaces, let alone over complex dune terrain.

This research also shows that a decline in Reynolds stress and related ejection and sweep activities toward the crest is driven by topographic forcing of flow streamlines. A recent study by Wiggs and Weaver (in review) found that sweeps and outward interactions were responsible for sand transport over an un-vegetated barchan dune. Although ejections were the most frequent activities, the less frequent sweep activities,

which have a greater contribution to momentum exchange (Lee and Black, 1993; Yue et a., 2007), were responsible for over two thirds of all observed sediment transport (Wiggs and Weaver, in review). The results presented here show that the ratio of Q2 ejections: Q4 sweeps is nearly balanced (i.e., close to 1) in flow on the lower stoss of the dune with a shift toward more ejections than sweeps (and less of both, overall) toward the crest. Exuberance values over the foredune were closer to zero at the toe and over the stoss of the dune whereas, at the crest, the exuberance values were closer to one. This indicates that Q2 and Q4 activity occur with greater frequency at the toe and along the stoss slope, while at the crest there is a greater frequency of Q1 and Q3 activities.

The highest frequency of ejection and sweep activities, along with the highest Reynolds stress values occurred at the toe and stoss slope measurement locations, respectively. Hypothetically, this may suggest that sediment entrainment and transport potential may be highest on the lower stoss slope, which would assist in ensuring sediment supply to the foredune, as suggested by others (e.g., Hesp et al., 2005; Walker et al., 2006; Walker et al., 2009). At the crest of the dune, the decline in Q2 and Q4 activity suggests a decrease in sediment entrainment potential and possible deposition in the crest region. Though it is unclear as to the role and influence the vegetation and vegetation canopy may have on the sediment transport and how it may influence or inhibit the sand grains in motion. As a result, this will affect the dune morphodynamics due to the greater turbulent shear stress and variability occurring at the toe, which in return promotes and allows sand transport. Whereas, at the crest there is a decrease in the potential of turbulent shear stress, which in returns promotes deposition. In return this will aid in the maintenance and growth of the dune.

2.7. Conclusion

This study provides novel information on turbulent airflow and near-surface Reynolds stress distributions in storm wind flow over a foredune. Reynolds stress decomposition was used to examine and quantify patterns in quadrant activity responsible for near-surface stress generation and sensitivities of these activities to changes in incident speed and flow direction. From this, implications for sediment transport and dune morphodynamics are discussed. The main conclusions are:

1. Increased near-surface Reynolds stress at the toe and lower stoss region enhances the frequency of stress generating Q2 ejection and Q4 sweep activity. Reynolds stresses were highest in the near-parallel flow above the stoss slope, where Q2 ejection and Q4 sweep activity frequencies were high and flow exuberance values were low.
2. At the crest, despite flow acceleration in this region, Reynolds stresses decrease due to increasing frequencies of Q1 and Q3 interaction activity, which contribute negatively to stress generation.
3. Changes in incident flow angle and speed affect turbulent flow properties and Reynolds stress distributions over the foredune. As flow angles become more onshore (by 13° to 22°) resultant speed along the stoss and at the crest increases, whereas a decrease is observed at the toe and in the lee of the dune. Reynolds stresses at the toe and lower stoss increase as incident flow becomes more onshore and as resultant speed increases, whereas, at upper stoss, crest, and lee locations Reynolds stress decreases. As Reynolds stresses increased there was an increase in Q2 (ejections) and Q4 (sweeps) activity. When Reynolds stresses

decreased there was a decrease in Q2 (ejections) and Q4 (sweeps) activity and a noticeable increase in Q1 (outward interactions) and Q3 (inward interactions) activity.

4. A flow exuberance effect is evident in flow over the foredune that controls the spatial distribution of Reynolds stress and related quadrant activities. Q2 ejection and Q4 sweep activity that contribute positively to Reynolds stress generation are most frequent at the foredune toe and stoss slope locations. It is believed that this reflects concave streamline curvature over the lower dune and the conveyance of these stress-generating activities toward the bed. Toward the crest, however, these stress-generating activities decline in frequency to increasing Q1 and Q3 interactions due to convex streamline curvature and flow acceleration in the crest region that suppresses turbulent motions. This decline in stress-generating turbulent activities and corresponding drop in time-averaged RS toward the crest suggests decreased sand transport potential and an increased tendency for deposition toward the crest. This flow exuberance effect was enhanced for more onshore flow angles suggesting an increased potential for sediment entrainment and transport over (and beyond) the dune during more onshore flows, most likely due to enhanced streamline compression and flow acceleration effects.

2.8. Acknowledgements

This research was supported by a Parks Canada Ecosystem Science Fund grant to RDA, JO, and IJW, an NSERC Special Research Opportunity Grant to RDA, IJW, BOB, an NSF and LSU Faculty Research grant to PAH, and Canada Foundation for Innovation

grants to IJW and JO. Valuable field assistance was also provided by Steven Namikas, Leah Olsen, Jeff Anderson, Jennifer Booth and Parks Canada Staff (Alan McGowan and Roger Steadman).

3.0. Turbulent Reynolds Stress, Quadrant Activities and Sand Transport Response over a Vegetated Foredune

3.1. Abstract

This study explores turbulent airflow behaviour, decomposed kinematic Reynolds stress (RS= -u' w') distributions, and corresponding sediment transport in near-surface airflow over a vegetated foredune at the Greenwich dunes, Prince Edward Island National Park, P.E.I., Canada. Coarse scale (1 Hz) sampling of three-dimensional velocity components by ultrasonic anemometers (0.2 m and 1.2 m) and sand transport intensity (0.014 m) via precise laser particle counters occurred at 4 locations over the dune. Wind conditions and sand transport were measured during the approach of a mid-latitude cyclone on 3-4 May 2010 generating storm force winds shifting from offshore to alongshore to obliquely onshore as wind speeds increased from 4 to > 20m s^{-1} at the crest. Reynolds decomposition of quasi-instantaneous fluctuating u' and w' signals into quadrant (Q) activities (i.e., Q1 outward interactions: u'>0, w'>0; Q2 ejections: u'<0, w'>0; Q3 inward interactions: u'<0, w'<0; Q4 sweeps: u'>0, w'<0) is explored to identify patterns of Reynolds stress (RS) signal distributions over the dune. Over dunes topographically forced streamline curvature effects alter quadrant activity distributions and, hence, near-surface RS generation by enhancing (at the toe) or inhibiting (at the crest) turbulent motions. This results in Q2 ejections and Q4 sweeps dominating stress generation on the beach, dune toe, and lower stoss slope, whereas, toward the crest, Q1 outward and Q3 inward interactions tend to dominate. Results show that RS generation and sand transport depend not only on location over the dune (via topographic forcing

effects on streamline curvature and flow stagnation/acceleration), but also on incident flow direction via topographic steering effects that alter the apparent ‘steepness’ of the dune to flow streamlines. Quadrant activity frequencies and flow exuberance are correlated to observed sand transport intensity to explore relations between the ejection-sweep phenomenon, topographic forcing effects, and resulting sand transport. Transport on the beach and lower stoss slope was driven predominantly by ejections and sweeps (> 60%, ejections + sweeps), while toward the crest it became dominated by outward and inward interactions (> 60 %, inward + outward interactions), likely due to increased frequency of streamwise gusts (+u’) and vertical lift (+w’) in topographically compressed flow. These findings challenge the current view in aeolian research that streamwise motions dominate sand transport over dunes and enhance our understanding of the effects of topographic forcing and streamline curvature on sand transport in air.

3.2. Introduction

The relationships between three-dimensional turbulent airflow, near-surface Reynolds stresses, and sand transport over aeolian dunes are poorly understood and relatively unexplored. This is partially due to the delay in availability of instrumentation to measure high frequency turbulent airflow and sediment transport and the uncertainty of the role that vertical velocity (w) plays in aeolian sand transport (Walker, 2006). Very recently, more interest has been placed on exploring relations between turbulent airflow and quasi-instantaneous sand transport through the examination of near surface Reynolds stresses (RS) and quadrant ‘activity’ decomposition (Chapman et al., in preparation; Wiggs and Weaver, in review). Wind tunnel research has shown that turbulent Reynolds

stress (RS) at the toe of a dune often exceed time-averaged, streamwise shear stress (ρu_*^2) due to microturbulent structures being conveyed towards the bed along a concave streamline (Wiggs et al., 1996; Walker and Nickling, 2002; 2003; Parsons et al., 2004). Towards the crest of a dune, surface stress often increases and is thought to be dominated by streamwise (u) accelerations that result directly from streamline compression, whilst vertical motions are inhibited by streamline convexity in this region (Wiggs et al., 1996; Walker and Nickling, 2002).

Reynolds stress represents the time-averaged vertical flux of the horizontal momentum at a point produced by fluctuations in the flow field. Statistically, RS is proportional to the covariance between orthogonal velocity components. Reynolds decomposition uses quasi-instantaneous deviations in horizontal and vertical velocity components (u' and w', respectively) to define quadrant activities that occur within high frequency turbulent RS signals. From this, four types of activities are identified: i) quadrant 1 (Q1) outward interactions ($u'>0$, $w'>0$), ii) quadrant 2 (Q2) ejections ($u'<0$, $w'>0$), which is fluid moving away from the bed where compared to the mean value the vertical component is moving faster and the streamwise is moving slower, iii) quadrant 3 (Q3) inward interactions ($u'<0$, $w'<0$), and iv) quadrant 4 (Q4) sweeps $u'>0$, $w'<0$), strong inrush of fluid moving towards the bed where compared to the mean value the vertical component is moving slower and the streamwise is moving faster (Figure 3.1) (Lu & Willmarth, 1973; Jackson, 1976). Upward Q2 (ejections) and downward Q4 (sweeps) contribute positively to RS and tend to dominate stress generation on flat surfaces and the lower stoss slope of a dune, whereas Q1 (outward interactions) and Q3 (inward interactions), that contribute negatively to RS generation, appear to dominate

near surface stress toward the crest of the dune (Chapman et al., in preparation; Wiggs and Weaver, in review).

In the fluvial literature, turbulent RS and decomposed quadrant activity have been associated with saltation and suspended sediment entrainment and transport (e.g., Jackson, 1976; Drake et al., 1988; Best, 1993; Robert et al., 1996, Best and Kostaschuk, 2002; Roy et al., 2004; Kostaschuk et al., 2008; Kostaschuk et al., 2009; Shugar et al., 2010) with buoyancy force playing a substantial role. In water, vertical velocity fluctuations (w') are more effective in entraining and transporting sediment because buoyancy effects are in the order of magnitudes greater than air. For example the density of quartz is 2650 kg m^{-3} and air density at sea level is 1.23 kg m^{-3}, therefore the density ratio for sand in air is approximately 2155:1 vs. 2.65:1 in water at standard temperature and pressure. Coherent microturbulent structures (e.g., low speed streaks, hairpin vortices, ejections, and sweeps) exist in turbulent boundary layer flow and generate high RS and contribute to sediment transport (Jackson, 1976; Drake et al., 1988; Best, 1993; Roy et al., 2004; Kostaschuk et al., 2008; Kostaschuk et al., 2009; Shugar et al., 2010). Low speed streaks of fluid lift up from the surface and evolve into an ejection (i.e., -u', +w') . Ejections either occur independently or in groups to give rise to bursting within the near-surface boundary layer (Jackson, 1976; Best, 1993). Strong downward inrushes of the fluid, known as sweeps (i.e., +u', -w'), impinge on the bed, entrains sediment and transport it at faster than average speeds (Drake et al., 1988).

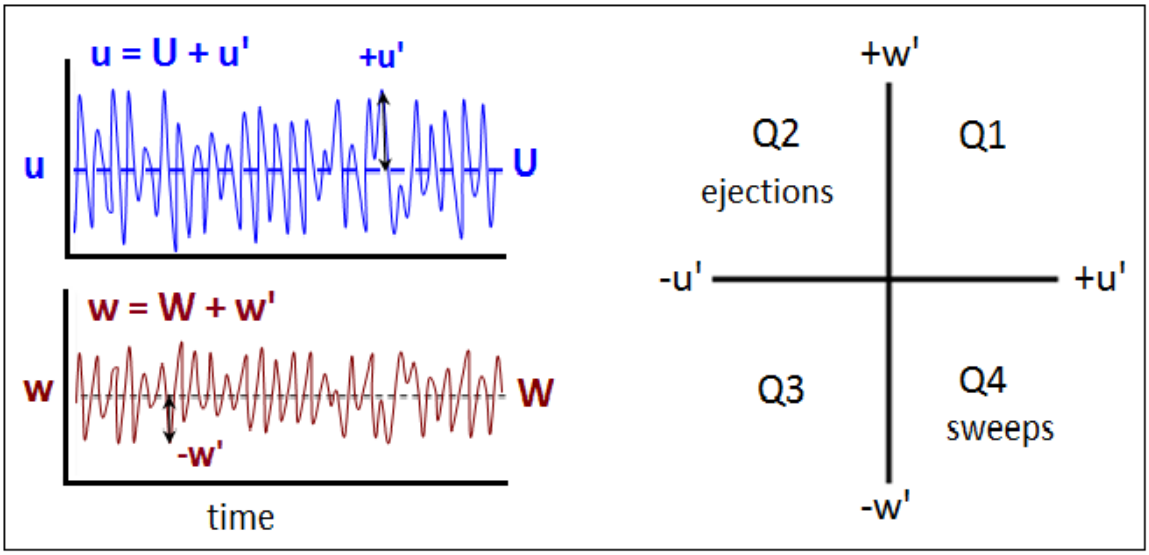

Figure 3.1: Turbulent velocity time series components plotted as quasi-instantaneous u' and w' quadrants where Q2 and Q4 activity typically dominate the Reynolds stress signal.

Recently, research has emerged on the relationships between turbulent airflow properties and sand transport over aeolian dunes (e.g., Baas, 2006; Livingstone et al., 2007; Lynch et al., 2009; Walker et al., 2009a; Walker et al, 2009b; Weaver and Wiggs, 2011; Baddock et al. 2011; Chapman et al., in preparation; Wiggs and Weaver, in review). Recent work over desert dunes in the Skeleton Coast, Namibia showed that ejection and sweep activities dominate at the toe of the dune (Wiggs and Weaver, in review) and, although ejections had a greater frequency of occurrence, sweep activities were responsible for more than 2/3 of the observed sand transport. Towards the crest of the dune, however, outward interactions were responsible for about 1/3 of the sediment transport (Wiggs and Weaver, in review).

Chapman et al. (in preparation, Section 2.0 of this thesis) found that ejection and sweep activities measured at 0.60 m and 1.66 m dominated at the toe and on the stoss slope of a foredune where kinematic RS was the greatest. Toward the crest there was a decrease in ejection and sweep activities and an increase in outward- and inward interaction activities, along with a decrease in RS (Chapman et al., in preparation, Section 2.0). The quadrant activity distribution is influenced by topographic forcing of flow streamlines (e.g., concavity, convexity) (Chapman et al., in preparation, Section 2.0). Although this study did not measure sand transport, it is hypothetically suggested that sand entrainment and transport may be greatest at the toe and along the stoss where ejection and sweep activities dominate and RS is high supplying sand supply to the foredune whereas, at the crest, there is a decrease in potential sediment entrainment and greater possibility for deposition.

This paper builds on previous work on three-dimensional airflow and RS distributions at the same study site as Chapman et al. (in preparation, Section 2.0) from a different field experiment and instrument deployment. Novel results are presented that aim to link observed sand transport to near-surface turbulent flow behaviour during a mid-latitude cyclone. The purpose of this paper is to quantify and examine measurements of turbulent airflow properties, Reynolds stress distributions and decomposed activities, and sand transport over a vegetated foredune via the following objectives:

1. To measure variations in quasi-instantaneous (1hz) near-surface three-dimensional velocity components (i.e., u ,v, w) and co-located sand transport intensity (grain counts) along a transect over a coastal foredune.
2. To examine relationships between near-surface airflow, decomposed quadrant activity structures (e.g., ejections, sweeps, inward/outward interactions) responsible for Reynolds stress generation and coincident sand transport.
3. To explain patterns in near-surface airflow dynamics, RS signal distributions, and observed sand transport.
4. To discuss implications for sand supply and transport patterns over foredunes.

3.3. Study Site

The study site is located on a stretch of foredune within the Greenwich Dunes in Prince Edward Island National Park on the north-eastern shores of Prince Edward Island (PEI), Canada (Figure 3.2). This site has hosted previous research on beach-dune airflow and sand transport dynamics (e.g., Hesp et al., 2005; Walker et al., 2006; Davidson-Arnott et al., 2008; Bauer et al., 2009; Bauer et al., 2009; Davidson-Arnott et al., 2009;

Davidson-Arnott and Bauer, 2009; Hesp et al., 2009; Walker et al., 2009a; Walker et al. 2009b; Delgado-Fernandez and Davidson-Arnott, 2011; Chapman et al. in preparation). The segment of foredune studied extends to approximately 9.8 m above mean sea level, has a stoss slope (windward slope) steepness of 21° to 27° and a crestline orientation of approximately ENE (~70°). The toe of the foredune had a small scarp of approximately 0.3 m, formed by a previous high water event that was fronted by an un-vegetated concave sand ramp that graded gently to the beach. The foredune fronts onto a low gradient, micro-tidal (~1 m range) beach with a low tide width of about 35 m. The beach is predominantly composed of quartz sand with an average diameter of 0.26 mm. The dune was vegetated by American beach grass (*Ammophlia breviligulata*) that, at the time of the experiment (May), was at the beginning of its growing season, where plant densities ranged from 10% to 40%. During the winter months this dune system is often covered in snow and fronted by shorefast ice.

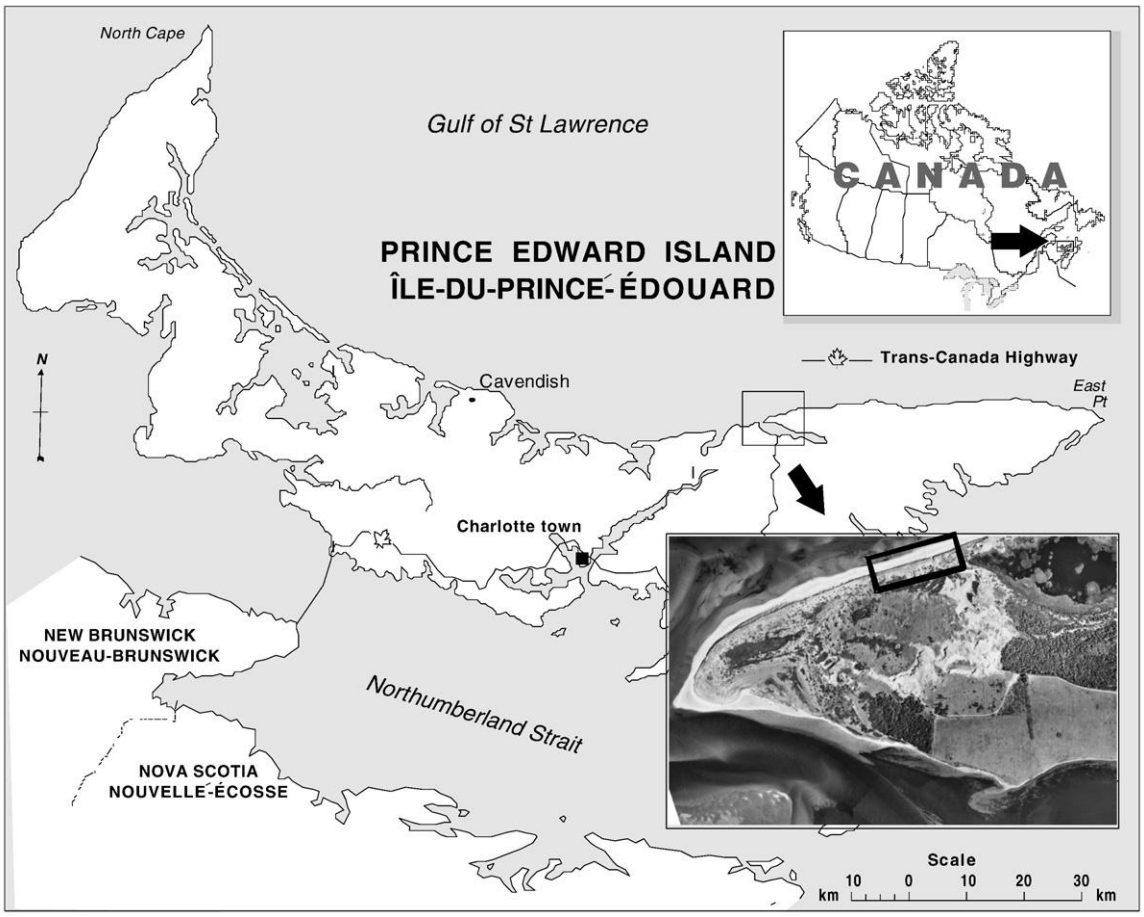

Figure 3.2: Location of study site.

Environment Canada meteorological data for 1995-2000 from Stanhope (~25 km to the southwest on the coast) show that the prevailing summer winds in the region are predominately from the southwest and are alongshore to offshore. While, these winds are frequent, they are often below sand transport threshold, while strong oblique to onshore winds from the north through northwest in the fall and winter are more competent for onshore transport and dune maintenance (Pearce and Walker, 2005; Hesp et al., 2005; Walker et al., 2006). Delgado-Fernandez and Davidson-Arnott (2010) found that a large portion of the total sediment flux over a 9 month period was moved by a few small to medium (8- 12 m s^{-1}) wind events and that the angle and fetch are more important than strong winds. Strong wind events saw wave scarping and foredune erosion instead of large amounts of sand transport (Delgado-Fernandez and Davidson-Arnott, 2010). During the winter months, which is the windiest season, was the least important for sand transport due to a frozen beach and snow/ice cover (Delgado-Fernandez and Davidson-Arnott, 2010).

The wind event examined here occurred between 2200 h AST on 3 May to 1400 h on 4 May 2010 and during the passage of a mid latitude cyclone. Wind direction shifted from offshore at 0050 h to alongshore where at around 0230 h it started to shift to obliquely onshore (Figure 3.3). Incident wind conditions on the beach measured at 3.82 m ranged from ~1.5 to >15 m s^{-1} and on the crest at 3.64 m ranged from ~4 to > 20 m s^{-1} (Figure 3.3). Rainfall occurred between 2200 h and 2330 h and active sand transport started at around 0050 h as the wind shifted from offshore to alongshore.

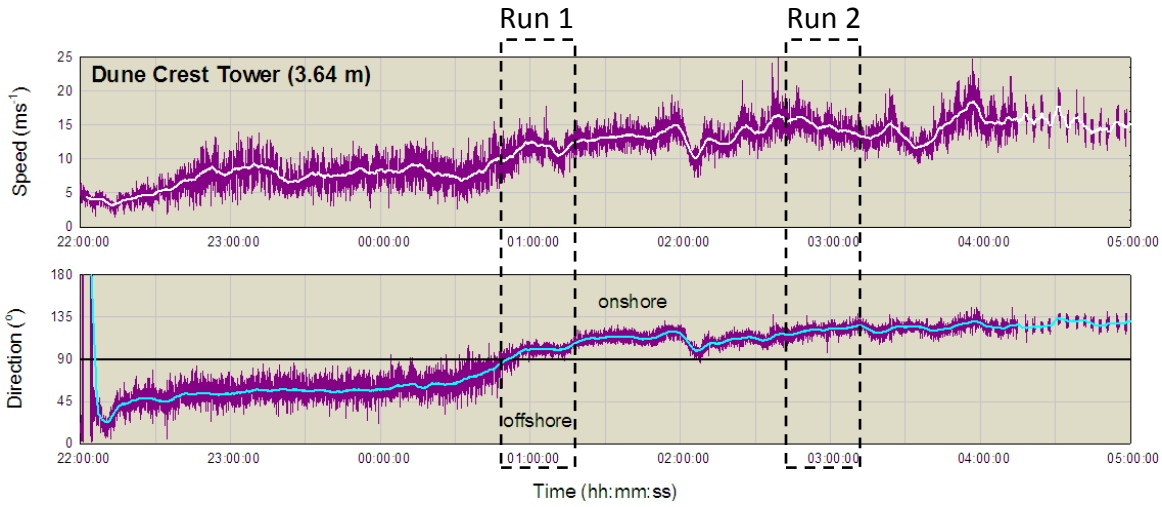

Figure 3.3: Time series representing the flow conditions direction, and speed from the crest tower (3.64 m) during the approach of a mid latitude cyclone on 3-4 May 2010.

3.4. Methods

3.4.1. Instrument Deployment

Three-dimensional velocity components (u, oriented alongshore; v, oriented off-on shore; w, vertical) were measured using Gill WindMaster 3-d ultrasonic anemometers at four different locations (beach, toe, stoss, and crest) and at some locations two different heights (near-surface at 0.20 m and upper flow at 1.2 m) along a shore-normal transect over the foredune (Figure 3.4). Two sonic anemometers were located at 0.20 m and 1.2 m on the beach, one sonic anemometer at 0.20 m at the foredune toe, one at 0.20 m on the stoss slope, and two at 0.20 m and 1.2 m at the crest of the dune. Instantaneous sand transport intensity was measured as grain counts using Wenglor (model #-YH08PCT8) Laser Particle counters with 8 cm sampling path length that were co-located with the sonic anemometer locations and were place below the vegetation canopy at 1.4 cm (Figure 3.5). Voltage outputs and pulse counts from sonic anemometers and laser particle counters, respectively, were sampled at 1 Hz by Onset Hobo Energy Pro data loggers with an onboard memory that was collected using a notebook computer. Instruments were oriented to true north and u-v axes were aligned to the underlying surface slope to reduce streamline misalignment to the sensor sampling plane (Walker, 2005). Data post processing rotated frames of reference such that the U axis became orientated into the dominant (alongshore) flow direction and V into the spanwise (on-off shore) axis. Pitch and yaw rotation was also applied to the data to correct for any remnant streamline misalignment effects as described below.

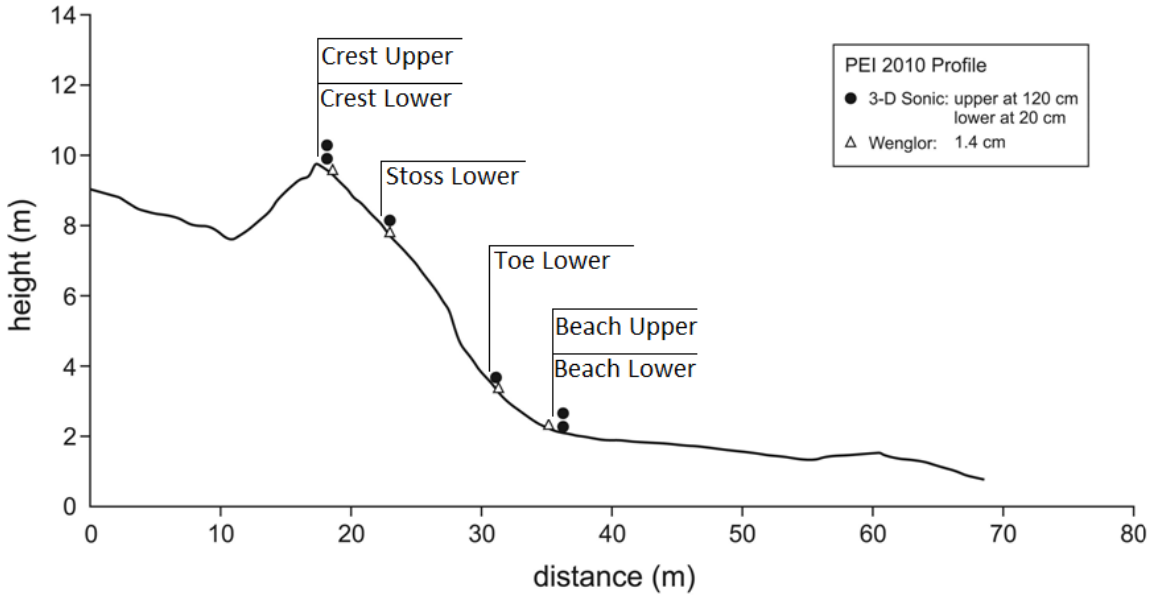

Figure 3.4: Profile of the dune system showing the location of the 4 stations.

Figure 3.5: Photograph of the study site. The transect ran from the beach to the crest of the dune and had a total of four different locations. The 3-D sonic anemometer stations at the beach and crest were located at two different heights, 1.2 m and 0.2 m, whereas, the 3-D sonic anemometer stations at the toe and the stoss were located at a height of 0.2 m. All stations were aligned with the underlying surface slope and each location had a co-located Wenglor Laser Particle counter at 1.4 cm.

3.4.2. Data Description and Analyses

The data explored in this paper consist of two 30-minute runs of 1 Hz continuous data recorded between 0050 h and 0310 h on 3-4 May 2010, yielding two datasets of up to 1800 coincident observations each (Table 3.1). A 30-minute period was chosen in order to obtain enough data points to thoroughly represent a quadrant activity distribution and to allow for sufficient representation of turbulent flow behaviour. The 30 minute runs were selected based on a consistent incident angle and resultant speed from consecutive 10 minute sub sections. The 10 minute sub sections were selected based on working instrumentation and periods without rain due to the fact that the Wenglors record rain drops. Throughout the experiment numerous instruments malfunctioned and it was a challenge to obtain sections with all working instrumentation. Run 1 (0050- 0120) had an average resultant speed (direction) of 7.84 m s^{-1} (-7°) at the upper beach and 7.59 m s^{-1} (-32°) at the upper crest location, where (0°= alongshore, -90°= onshore, 90°= offshore). Run 2 (0240- 0310) had upper wind speed (direction) of 10.21 m s^{-1} (-20°) at the upper beach and 11.15 m s^{-1} (-47°) at the upper crest location.

Three-dimensional velocity data were rotated post-measurement to orient the streamwise (u) component into the dominant flow direction (e.g., alongshore to the west) and then rotated for yaw and pitch correction in order to rectify any remaining sensor misalignment to local streamlines (Roy et al., 1996; van Boxel et al., 2004; Walker, 2005). The following equation was used for the yaw correction:

$$u_1 = u_x \cos\alpha + v_z \sin\alpha \tag{3.1}$$

$$w_2 = -u_x \sin\varphi + w_y \cos\varphi \tag{3.2}$$

$$\alpha = \arctan\left(\frac{V_z}{U_x}\right) \tag{3.3}$$

where u_1 and v_1 are the yaw corrected values, alpha (α) is the time averaged angle for flow, and U and V indicate the time averaged values (Walker, 2005). This correction will adjust the u component toward the mean flow vector. The following equation was used for the pitch correction:

$$u_2 = u_x \cos\varphi + w_y \sin\varphi \tag{3.4}$$

$$w_2 = -u_x \sin\varphi + w_y \cos\varphi \tag{3.5}$$

$$\varphi = \arctan\left(\frac{W_y}{U_x}\right) \tag{3.6}$$

where u_2 and w_2 are pitch rotated values from the previous equations 3.1-3.3, phi (φ) is the angle of the incoming streamline, and U and W indicate the time averaged values (Walker, 2005). Streamline curvature was determined through comparison of calculated streamline angles (from equation 3.6) to underlying surface slope angles (Table 3.1).

The rotated pitch values were used to derive the quasi- instantaneous prime values, which were then used to establish the kinematic Reynolds stresses (RS_k) using the following equation:

$$RS_k = -\overline{u'w'} \tag{3.7}$$

where Reynolds stresses represent the time-averaged vertical flux of horizontal momentum at a point produced by concurrent oscillations of opposing velocity components.

Reynolds stress decomposition was performed on the rotated three-dimensional velocity datasets using the u and w components to produce decomposed RS activity quadrant plots for runs 1 and 2. These plots visualize the frequency distribution of activities that dominate RS generation at the measurement point. Quadrant activity frequencies shown in brackets (see Figures. 3.6 and 3.7 and Tables 3.1 and 3.2) represent

only significant stress activities that exceed a threshold (H) value of one standard deviation of RS_k, as is commonly recommended (Lu and Wimarth, 1973).

A range of summary statistics was calculated for both turbulent airflow properties and instantaneous sand transport intensity observations. For airflow properties u, v, and w, the time average was calculated (U,V,W), standard deviation (σ), minimum, maximum, resultant vector (UV) magnitude, and streamwise and vertical flow steadiness, using a coefficient of variation, $CV_{u \text{ or } w}$ as follows:

$$CV_u = \frac{\sigma_u}{U} \tag{3.8}$$

Flow exuberance (EX_{FL}) describes the shape of the quadrant frequency distribution through a ratio of total Q1 and Q3 activities to Q2 and Q4 activities (Shaw et al., 1983; Yue et al., 2007):

$$Exuberance_{Flow}(EX_{FL}) = \frac{Quadrant\ 1 + Quadrant\ 3}{Quadrant\ 2 + Quadrant\ 4} \tag{3.9}$$

As such, the flow exuberance value expresses the shape of the activity distribution or, physically, the ratio of negative to positive contributions to Reynolds stress generation. When EX_{FL} is close to one, it represents an even distribution of activities spanning all four quadrants (i.e., a circular quadrant plot) whereas, when EX_{FL} approaches zero, it indicates a dominance of Q2 ejection and Q4 sweep activities in the distribution (i.e., a skewed elliptical quadrant plot as is common in strongly sheared flows).

Measurements of sand transport intensity (grain counts per second) were lagged by 1 second from velocity measurements to conform with recent research that has shown a one to two second lag between flow changes and saltation response (e.g., Butterfield, 1991; Stout and Zobeck, 1997). A 2 second lag was explored though the results were extremely similar to a 1 second lag. Summary statistics for sand transport intensity

included minimum, maximum, standard deviation (σ), and transport exuberance (EX_{TR}) were calculated. A new quantity, termed the transport exuberance (EX_{TR}), was developed to describe the ratio between the total count of observed sand grains moved by Q1 and Q3 activities to that of Q2 and Q4 activities responsible for sand transport and is defined as follows:

$$Exuberance_{Transport}(EX_{TR}) = \frac{(Quadrant\ 1 + Quadrant\ 3) + 1}{(Quadrant\ 2 + Quadrant\ 4) + 1} \tag{3.10}$$

When the transport exuberance value is less than one Q2 ejection and Q4 sweep-style activities dominate sand transport, whereas when the value is greater than one Q1 outward- and Q3 inward-interaction activities dominate. Sand intermittency (γ_p) values were calculated using the approach of Stout and Zobeck (1997) whereby intermittency describes the portion of time that sand transport is active. Intermittency values range between 0 and 1, where 1 indicates constant sand transport and 0 indicates no transport over the period of observation (Stout and Zobeck, 1997).

Table 3.1: Summary of the flow properties: incident flow angle (IFA) (degrees), resultant speed (m s^{-1}), total kinetic energy (TKE) (m^2s^{-2}), Reynolds stress (RS) (u'w'), and flow exuberance ((Q1+Q3)/(Q2+Q4)). Observed values were used for U,V, and W, resultant speed and TKE, whereas, rotated values were used for the RS and IFA.

	Beach Lower (0.20 m) (+4°)	Beach Upper (1.2 m) (+4°)	Toe Lower (0.20 m) (+24°)	Stoss Lower (0.20 m) (+23°)	Crest Lower (0.20 m) (+2°)	Crest Upper (1.2 m) (+2°)
Run 1 (00:50- 01:20)						
Flow Angle (°)	-7	-7	-9	-20	-32	-20
U [CV_u]	6.92 [0.16]	7.78 [0.15]	5.96 [0.25]	3.67 [0.29]	6.42 [0.19]	9.68 [0.15]
V	-0.88	-0.96	-0.97	1.49	-4.06	-3.70
UV	6.98	7.84	6.04	4.05	7.59	10.36
W [CV_w]	-0.45 [-0.96]	0.27 [1.05]	-0.21 [-6.76]	0.017 [16.50]	0.42 [0.68]	0.59 [0.56]
Streamline angle (°)	0	6	26	22	6	6
TKE	0.99	1.06	3.72	1.56	1.65	2.21
RS	0.25	0.01	0.10	0.088	-0.38	-0.39
Run 2 (02:40- 03:10)						
Flow Angle (°)	-18	-20		-44	-47	-39
U [CV_u]	7.47 [0.184]	9.61 [0.14]		5.31 [0.20]	7.62 [0.17]	11.00 [0.13]
V	-2.45	-3.47		-5.12	-8.14	-8.80
UV	7.86	10.21		7.38	11.15	14.09
W [CV_w]	-0.35 [-1.61]	0.43 [0.56]		-0.32 [-1.00]	1.36 [1.57]	1.70 [0.20]
Streamline angle (°)	1	7		26	12	11
TKE	1.72	1.42		1.22	1.57	1.60
RS	0.35	-0.028		0.23	-0.18	-0.30

3.5. Results

3.5.1. Quadrant Activity Distributions and Reynolds Stress

Quadrant activity distribution plots changed with height and location over the dune, along with variations in incident flow angle (0°= alongshore, -90°=onshore, 90°= offshore) and resultant speed (Figures 3.6 and 3.7). Early in the observation period (run 1, Figure 3.6), the quadrant plots were more compact (i.e., less scatter in the distribution), whereas during faster, more onshore flow (run 2, Figure 3.7) the plots show more scatter in both u' and w' axes.

At the beach, toe, and stoss sampling locations, quadrant activity distributions showed a clear skewness toward Q2 ejection and Q4 sweep activities. Upper flow at the beach during runs 1 and 2 showed comparatively flat w' distributions and similar frequencies of all quadrant activities reflecting more isotropic turbulence(Figures 3.6 and 3.7 and Table 3.2). During faster and more onshore incident flow (Run 2), flow behaviour at the crest location showed increased scatter in Q1 and Q3 interactions, but a decrease in the range of u', whereas, at the lower beach (0.20 m)and stoss locations there was an increase in range of scatter in Q2 and Q4 activity. Total Q2 ejection and Q4 sweep activity frequencies remain similar between runs 1 and 2 for all locations, along with the significant activities exceeding the threshold H value of $>1\sigma$ in RS_k (Table 3.2).

Flow exuberance values were typically lowest (< 1) at the beach, toe, and stoss locations, which suggests that Q2 and Q4 activities dominated RS generation on the lower windward slope of the dune (Figure 3.6 and 3.7 and Table 3.2). As faster and more onshore flow occurred (run 2), flow exuberance values at the stoss location continued to decrease (Table 3.2). Flow exuberance was largest (> 1) at the upper (1.2 m) and lower

(0.20 m) crest locations where the quadrant activity distribution is skewed between Q1 and Q3, which suggests that Q1 and Q3 dominated RS generation on the upper windward slope of the dune (Figure 3.6 and 3.7 and Table 3.2). These results are consistent with Chapman et al. (in preparation) findings on the 'flow exuberance effect' where the flow exuberance was lowest at the toe and stoss locations and greatest at the crest locations. Therefore, along the beach, toe, and lower portion of the stoss slope Q2 and Q4 activities contribute positively to momentum flux towards the bed with resulting high RS values (greatest on the beach), whereas at the crest Q1 and Q3 contribute negatively to momentum flux and low resulting RS values.

Table 3.2: Summary of quadrant activity counts, grain counts, intermittency, and flow and transport exuberance. Values located within the brackets indicate significant values calculated from the significant quadrant activities (1 standard deviation removed).

	Quadrant Counts	Grain Counts	Intermittency	Flow Exuberance	Transport Exuberance
Run 1					
Beach	Q1: 319 (3)	Q1: 131249 (1747)	0.17		
	Q2: 747 (38)	Q2: 222921 (6630)	0.35		
	Q3: 222 (5)	Q3: 70843 (1914)	0.11	0.43 (0.083)	0.47 (0.11)
	Q4: 512 (58)	Q4: 203943 (25225)	0.28		
	Total: 1800 (104)	Total: 628956 (35516)	Total: 0.91		
Toe	Q1: 481 (0)	Q1: 154497 (0)	0.23		
	Q2: 753 (0)	Q2: 208623 (0)	0.38		
	Q3: 177 (10)	Q3: 53361 (4057)	0.09	0.59 (0.63)	0.62 (0.51)
	Q4: 355 (16)	Q4: 128796 (7959)	0.18		
	Total: 1766 (26)	Total: 545277 (12016)	Total: 0.87		
Stoss	Q1: 378 (34)	Q1: 1 (0)	0.00056		
	Q2: 588 (65)	Q2: 6 (0)	0.0028		
	Q3: 379 (10)	Q3: 2 (0)	0.0011	0.73 (0.29)	0.20 (0.17)
	Q4: 455 (89)	Q4: 13 (5)	0.0056		
	Total: 1800 (198)	Total: 22 (5)	Total: 0.01		
Crest	Q1: 654 (146)	Q1: 583 (291)	0.12		
	Q2: 194 (1)	Q2: 40 (0)	0.011		
	Q3: 698 (131)	Q3: 37 (1)	0.013	3.05 (92.33)	7.31 (293)
	Q4: 250 (2)	Q4: 44 (0)	0.01		
	Total: 1796 (280)	Total: 704 (292)	Total: 0.15		
Run 2					
Beach	Q1: 374 (5)	Q1: -	-		
	Q2: 814 (13)	Q2: -	-		
	Q3: 172 (12)	Q3: -	-	0.44 (0.18)	-
	Q4: 440(80)	Q4: -	-		
	Total: 1800 (110)	Total: -	Total: -		
Toe	Q1: -	Q1: -	-		
	Q2: -	Q2: -	-		
	Q3: -	Q3: -	-	-	-
	Q4: -	Q4: -	-		
	Total: -	Total: -	Total: -		
Stoss	Q1: 275 (9)	Q1: 756 (159)	0.13		
	Q2: 636 (115)	Q2: 884 (145)	0.22		
	Q3: 274 (4)	Q3: 308 (16)	0.09	0.45 (0.058)	0.46 (0.28)
	Q4: 594 (109)	Q4: 1417 (481)	0.25		
	Total: 1779 (237)	Total: 3365 (801)	Total: 0.69		
Crest	Q1: 676 (139)	Q1: 77268 (2553)	0.39		
	Q2: 183 (1)	Q2: 927 (34)	0.1		
	Q3: 724 (132)	Q3: 2283 (452)	0.4	4.12 (18.07)	3.78 (19.78)
	Q4: 157 (14)	Q4: 1592 (117)	0.09		
	Total: 1740 (286)	Total: 82070 (3156)	Total: 0.98		

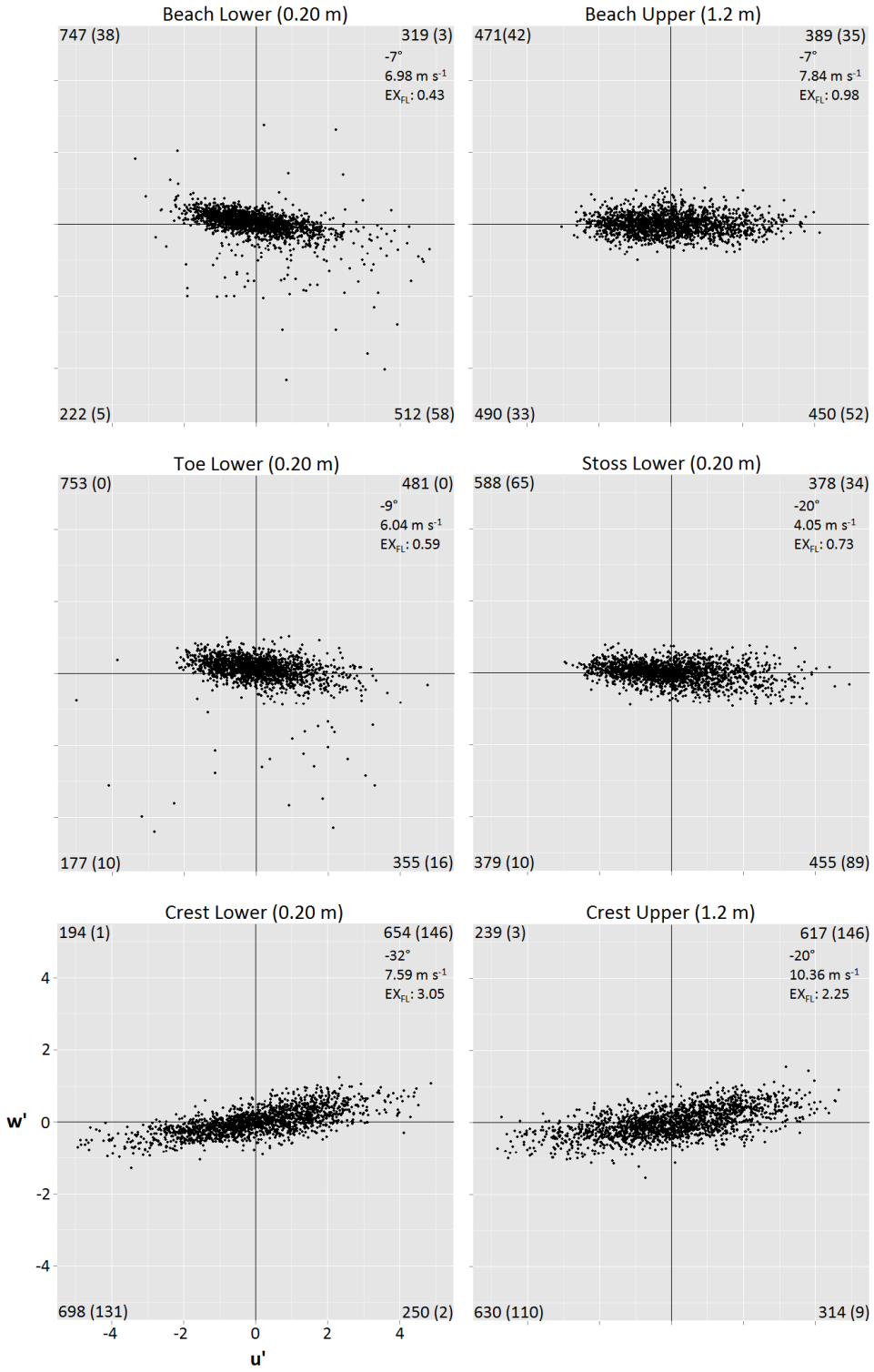

Figure 3.6: Run 1 quasi instantaneous (1Hz) quadrant plots for 30 minute run (n=1800) occurring at 0050 - 0120 h on 4 May 2010 during the approach of a mid latitude cyclone. The top right hand corner displays the incident flow angle (0= alongshore, -90= onshore, 90= offshore), resultant speed, and flow exuberance value (EX_{FL}). For each quadrant, values for total activity count and (significant activity counts that exceeded H>1 SD) are shown.

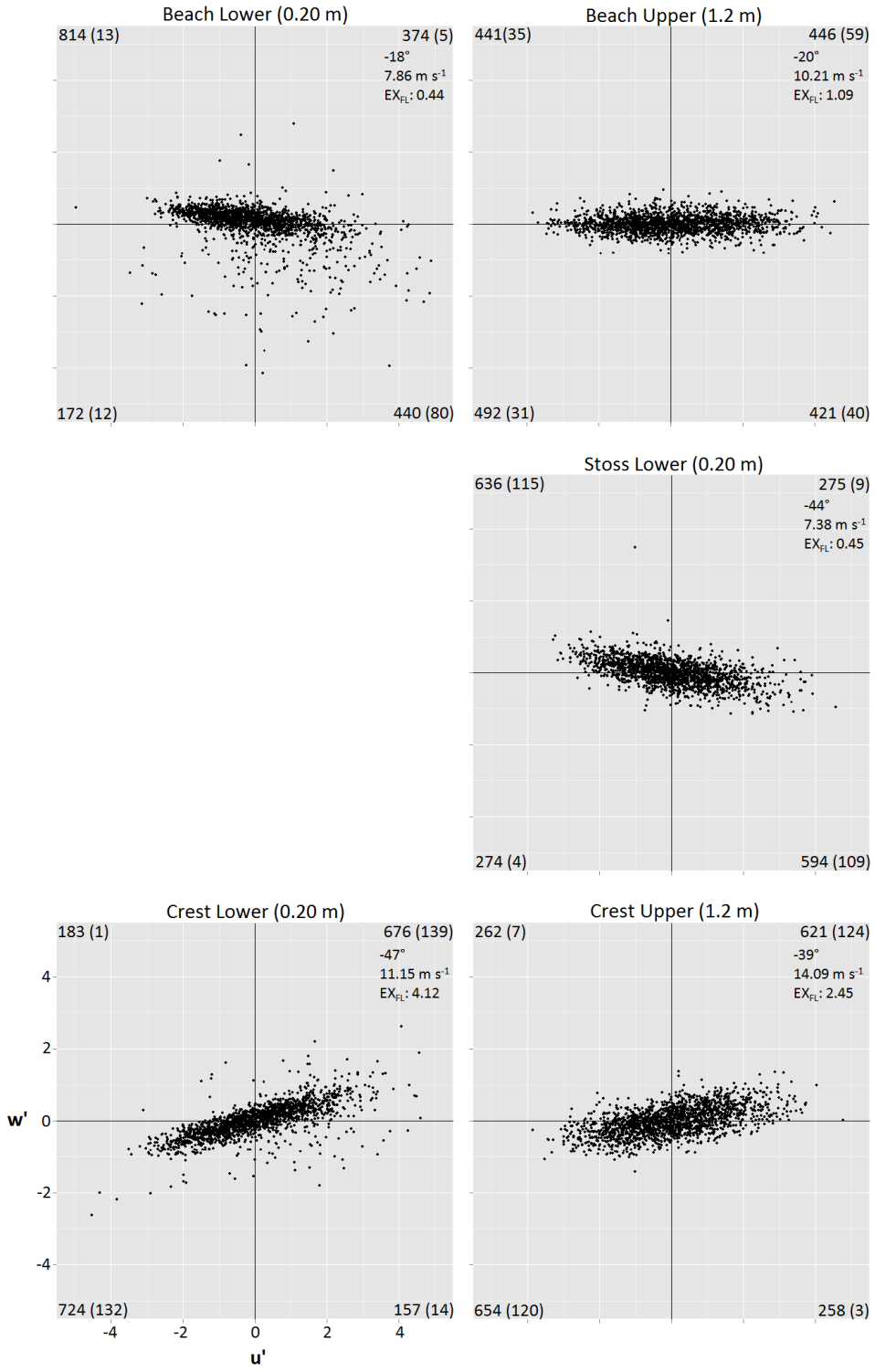

Figure 3.7: Run 2 quasi instantaneous (1Hz) quadrant plots for 30 minute run (n=1800) occurring at 0240 - 0310 h on 4 May 2010 during the approach of a mid latitude cyclone. The top right hand corner displays the incident flow angle (0= alongshore, -90= onshore, 90= offshore), resultant speed, and flow exuberance value (EX_{FL}). For each quadrant, values for total activity count and (significant activity counts that exceeded H>1 SD) are shown. Toe lower location missing due to instrument malfunction.

3.5.2. Sand Transport Intensity

During run 1, active transport occurred at all locations (beach, toe, stoss, and crest) on the dune. Sand transport intensities were greatest directly after the flow shifted from offshore to alongshore (0050- 0120 h), where a total of $1.17x10^6$ sand grains were moved over the 30-minute period. The beach and the toe of the dune experienced the greatest sand transport with $6.29x10^5$ and $5.45x10^5$ sand grains moved, respectively (Table 3.2). The beach had a maximum grain count, or transport activity, of 1200 sand grains in one second, whereas, the maximum activity at the toe of the dune was 1262 sand grains per second. On the stoss slope a dramatic decrease in sand transport was observed with only a total of 22 sand grains being moved and a maximum grain count of 3 sand grains per second over the 30-minute run. By comparison, the crest of the dune had 32 times the observed total sand transport on the stoss with a total of 704 grains moved over the 30-minute run and had a maximum transport activity of 14 sand grains per second. Intermittency values at the beach (0.91) and toe (0.87) confirm almost continuous sand transport during the 30-minute run (Table 3.2). At the stoss and crest of the dune intermittency values decreased to 0.01 (stoss) and 0.15 (crest) indicating discontinuous sand transport during the 30- minute run (Table 3.2).

Run 2 (0240- 0310 h) lacked instantaneous sand transport data for the beach and toe locations dune to an instrumentation malfunction. Sand transport intensity increased by 3.6 times between the stoss and the crest locations as near-surface wind speeds increased and direction became obliquely onshore. A total of $1.54x10^4$ sand grains were moved over the 30 minute period, while on the stoss slope a total of 3365 grains were moved with a maximum sand transport activity of 80 grains per second (Table 3.2). Sand

transport at the crest of the dune increased from the stoss with a total of $1.21x10^4$ sand grains moved and a maximum transport activity of 98 grains per second (Table 3.2). Intermittency values on the stoss (0.69) indicate that sand transport was relatively continuous for run 2 (Table 3.2). The crest of the dune experienced almost continuous sand transport throughout the 30-minute run with an intermittency value of 0.98 (Table 3.2).

3.5.3. Quadrant Activity and Sand Transport

Sand transport and quadrant activity distributions for run 1 were dominated by Q2 ejection and Q4 sweep activities at the beach, toe, and stoss locations (Table 3.2 & 3.3). Wind flow was directly alongshore and observed RS values were typically the highest. Generally, Q2 ejection and Q4 sweep activities drove sand transport at the beach and toe of the foredune. On the stoss slope, Q2 ejection and Q4 sweep activities also dominated, yet there was a substantial decrease in sand transport by two orders of magnitude (10^3 to 10^5 times less) in comparison to the beach and toe (Table 3.2 & 3.3). Transport exuberance values were also typically low on the stoss indicating that Q2 ejection and Q4 sweep activities dominated transport activity (Table 3.2). The beach, toe, and stoss locations experienced Q2 ejection and Q4 sweep activities responsible for moving >60 % of the sand (Table 3.3). Q1 outward interactions and Q3 inward interactions dominated sand transport at the crest of the dune where sand transport increased 32 times over that at the stoss sampling location (Table 3.2). Transport exuberance values were generally high at the crest indicating that Q1 and Q3 interaction activities dominated observed transport (Table 3.2) and were responsible for moving 88% of sand grains (Table 3.3).

Identification and use of only significant quadrant activities (i.e., those that exceed the threshold H value of $>1\sigma$ in RS_k) was instrumental in demonstrating that Q4 sweep activities dominated sand transport at the beach, toe, and stoss locations and Q1 outward interactions at the crest (Table 3.3). Significant Q4 sweeps moved more than >65 % of the sand at the beach, toe, and stoss for both runs 1 & 2 (Table 3.3). Significant Q1 outward interactions were responsible for 100% of the sand grains moved at the crest for both runs 1 & 2 (Table 3.3).

Similar to run 1, sand transport and quadrant activity distribution for run 2 were dominated by Q2 ejection and Q4 sweep activities at the stoss location. The wind flow was obliquely onshore and observed RS values were typically the highest. Generally, ejection and sweep activities dominated the sand transport along the stoss of the foredune and, combined, were responsible for moving 71% of the sand (Table 3.3). Transport exuberance values at the stoss were typically low indicating that Q2 ejection and Q4 sweep activities dominated observed transport (Table 3.2). Q1 and Q3 interaction activities dominated sand transport at the crest of the foredune and, combined, were responsible for moving 79% of the sand (Table 3.3). Transport exuberance values were generally high corresponding with high flow exuberance values at the crest indicating that Q1 and Q3 interaction activities dominated (Table 3.2). Significant Q4 sweeps and Q1 outward interactions dominated observed sand transport with Q4 moving 60% of the sand at the stoss location and Q1 moving 81% of the sand at the crest (Table 3.3).

For both runs 1 and 2 transport intermittency values were highest in the dominating quadrants. For example, for run 1 at the toe, beach, and stoss locations intermittency values were greatest in Q2 and Q4, whereas at the crest intermittency

values were greatest for Q1 and Q3 activities (Table 3.2). For run 2, intermittency values at the stoss location were highest for Q2 and Q4, whereas at the crest of the dune, intermittency values were highest for the dominating Q1 and Q3 activities (Table 3.2).

For sand transport though, RS values did not correspond well with observed transport intensity or total sand counts. High values of total grain counts occurred with a variety of different RS values and with the dominating quadrant activities over the foredune (beach, toe, stoss, crest) throughout runs 1 & 2. For example, at the crest low RS values were observed (due to dominance of Q1 and Q3 activities in the signal) yet observed sand transport was higher than on the stoss where RS values were higher (Table 3.2). At the crest Q1 and Q3 dominated with a negative RS, though Q1 and Q3 contribute negatively to momentum change they were still responsible for sand transport. This is possibly due to activities occurring up wind or that +u' motions (streamwise gusts) may play a greater role than initially expected. It must be noted that the u' and w' are not the up and down motions of the u and w. Table 3.1 provides the average U and W values over the 30 minute runs.

Table 3.3: Summary of flow exuberance and Reynolds stress from the lower (0.20 m) 3-D sonic anemometer stations and percent of transport per quadrant over the dune. Values located within brackets were calculated from significant quadrant activities (1 standard deviation removed).

	Beach		Toe		Stoss		Crest	
Run 1								
EX_{FL}	0.43 (0.083)		0.59 (0.62)		0.73 (0.29)		3.04 (92.33)	
RS	0.25		0.10		0.088		-0.38	
% of	Q1:	21 (5)	Q1:	28 (0)	Q1:	5 (0)	Q1:	83 (100)
Transport	Q2:	35 (19)	Q2:	38 (0)	Q2:	27 (0)	Q2:	6 (0)
per	Q3:	11 (5)	Q3:	10 (4)	Q3:	9 (0)	Q3:	5 (0)
Quadrant	Q4:	32 (71)	Q4:	24 (66)	Q4:	59 (100)	Q4:	6 (0)
Run 2								
EX_{FL}	0.43 (0.18)		-		0.45 (0.058)		4.11 (18.07)	
RS	0.35		-		0.23		-0.48	
% of	Q1:	-	Q1:	-	Q1:	22 (20)	Q1:	60 (81)
Transport	Q2:	-	Q2:	-	Q2:	26 (18)	Q2:	8 (1)
per	Q3:	-	Q3:	-	Q3:	9 (2)	Q3:	19 (14)
Quadrant	Q4:	-	Q4:	-	Q4:	45 (60)	Q4:	13 (4)

3.6. Discussion

3.6.1 Flow Behaviour and Turbulent Quadrant Activity Responses

Figure 3.8 generalizes the different responses in streamline behaviour, flow stability, flow acceleration, RS and quadrant activity distributions over the dune. Previous work by Chapman et al. (in preparation, Section 2.0 in this thesis) and Wiggs and Weaver (in review) has shown that topographic forcing of flow over dunes influences turbulent quadrant activity distributions and, thus, near-surface RS generation. Flow exuberance generally decreases on the lower windward slope of a dune in response to flow stagnation and concave streamline curvature, which conveys turbulent structures toward the bed and results in an increase in RS at the dune toe (Wiggs et al., 1996). In this study, this is attributed to an increase in Q2 ejection and Q4 sweep activities on the beach and at foredune toe. Conversely, toward the crest there is an increase in flow exuberance (i.e., more Q1 and Q3 interactions) and a corresponding decrease in RS near the surface, which relates to streamline compression and resulting suppression of turbulence in the crest region (Wiggs et al. 1996, Wiggs and Weaver, Chapman et al. in preparation). The shift in Q2 ejection and Q4 sweep activities dominated stress generation and low exuberance values at the toe of the foredune to an increasing negative stress contributions from Q1 and Q3 activities at the crest and higher exuberance values is known as the ‘flow exuberance effect’ (Chapman et al. in preparation).

Observed differences in flow properties and RS generation result from topographic forcing effects. Areas of high Reynolds stress (beach, toe, and stoss locations) exhibit a higher frequency of Q2 ejection and Q4 sweep activity influenced by streamline curvature (Chapman et al. in preparation; Wiggs and Weaver, in review). For example, concave streamlines at the toe of the dune cause a destabilization in the flow via

conveyance of turbulent structures towards the bed, which results in an increase in shear stress generation (Wiggs et al., 1996; Walker and Nickling, 2002) (Figure 3.8 a). Convex streamlines at the crest promote stabilization in the flow through the suppression of vertical motions (i.e., reduced vertical velocity fluctuations w') (Wiggs et al., 1996; Hesp et al., 2009; Walker et al. 2009b) (Figure 3.8 a). Although data in this paper were obtained at a coarser temporal scale than Chapman et al. (in preparation) (1 Hz vs. 32 Hz), the pattern in RS generating signals (and quadrant activity distributions generally) are consistent with their findings.

3.6.2. Interactions Between Turbulent Flow and Sand Transport

Observations of near-surface Reynolds stress patterns, decomposed quadrant activities, and corresponding saltation intensity counts provide a basis for discussing the relations between near-surface turbulent activities and sand transport patterns over aeolian dunes. Fluvial research suggests that Q2 ejection and Q4 activities are responsible for the majority of saltation and suspended sediment transport over subaqueous dunes with sweeps providing the most momentum for entrainment and transport (e.g., Jackson, 1976; Drake et al., 1988; Best 1993; Robert et al., 1996; Venditti and Bennett, 2000; Best and Kostaschuk, 2002; Kostaschuk et al., 2008; Kostaschuk et al., 2009; Shugar et al., 2010). In this study, Q2 ejection and Q4 sweep activities that contribute positively to RS generation had the greatest frequency in near-surface flow over the beach, toe, and stoss locations of the foredune and declined by 2.4 to 3.9 times for Q2 and 1.4 to 3.8 times for Q4 at the crest. These ejection and sweep activities were responsible for >60% of transport occurring at the beach, toe, and stoss for both runs 1 and 2(Table 3.3). What is

not understood is the potential role that the vegetation and the vegetation canopy plays in sand transport and how it enhances or inhibits sand grain motions.

Ejection and sweep activities dominate the RS signals and appear to drive sand transport at the beach, toe, and stoss locations (Figure 3.8b and c). Flow interaction activities (Q1 and Q3), meanwhile, dominate the RS signal and sand transport at the crest of the dune (Figure 3.8 b and c). Significant Q4 sweep activities at the beach, toe, and stoss locations and Q1 outward interactions at the crest dominated in the sand transport suggesting that not only do positive streamwise velocity variations (i.e., +u') play a significant role in sand transport as is known (e.g., Wiggs et al., 1996; Walker and Nickling, 2002; Parsons et al., 2004), but also vertical velocity contributions to the RS signal (either + or -w') are important. Though proportionately smaller in magnitude, this suggests that vertical velocity contributions play a greater role in aeolian sediment transport (via notable contributions to turbulent RS) than previously believed. This complements and expands on previous findings that have suggested that vertical velocity fluctuations, most notably upward 'lift' force, assist in initiating and maintaining sand transport over the dune (Wiggs et al. 1996; Walker and Nickling; 2002; 2003; Parsons et al., 2004; Walker et al., 2006).

This paper introduces the concept of 'transport exuberance' (EX_{TR}), or the ratio between the total count of observed sand grains moved by Q1 and Q3 activities to that of Q2 and Q4 activities responsible for observed sand transport. Transport exuberance values indicated that Q2 ejection and Q4 sweep activities drive sand transport at the beach, toe, and stoss locations, whereas, Q1 and Q3 dominated transport at the crest of the dune (Figure 3.8 c). Thus, a transport exuberance effect occurs whereby there is a

shift from transport driven by positive momentum contributions (Q2 and Q4) on the beach and lower dune to that driven by negative momentum contributions toward the crest. This reflects concave streamline curvature over the lower dune slope and toe region that conveys turbulent RS generating signals (ejection and sweep activities) toward the bed (Figure 3.8 a-c). Convex streamline curvature at the crest promotes a shift toward activities that contribute negatively to RS generation (Q1 outward- and Q3 inward interactions) yet are still capable of transporting sand due to coincident increases in streamwise velocity variations (u') (Figure 3.8 a-c). This transport exuberance effect directly reflects the pattern in flow exuberance outlined in Chapman et al. (in preparation, Section 2.0). It must be noted that a spatial and temporal lag is present between the turbulent flow and the sand transport due to the limitations of instrument positions providing only a snapshot of 'activity' signatures. In order to try and minimize the spatial and temporal lag a 1 second lag was applied to the sand transport data, though effective up wind conditions may still be responsible for some of the sand grain movement.

As flow moves along the beach and approaches the foredune toe it experiences streamline concavity, deceleration, and an increase in RS conveyance of turbulent structures towards the bed, whereas at the stoss of the dune streamlines are parallel with the surface (Figure 3.8 a). Ejection and sweep activities dominate the flow and transport at the beach, toe, and stoss, where time-averaged RS values were high and EX_{FL} and $EX_{TR}<1$ (Figure 3.8 b-c). At these locations sweep activities transported the greatest number of sand grains over the 30 minute runs. The crest of the dune experiences flow stabilization as flow accelerates due to streamline convexity (Figure 3.8 a). Outward and inward interactions dominated the flow and transport at the crest, where time-averaged

RS values were low and EX_{FL} and EX_{TR}>1 (Figure 3.8 b-c). At this location outward interactions transported the greatest number of sand grains over the 30 minute runs.

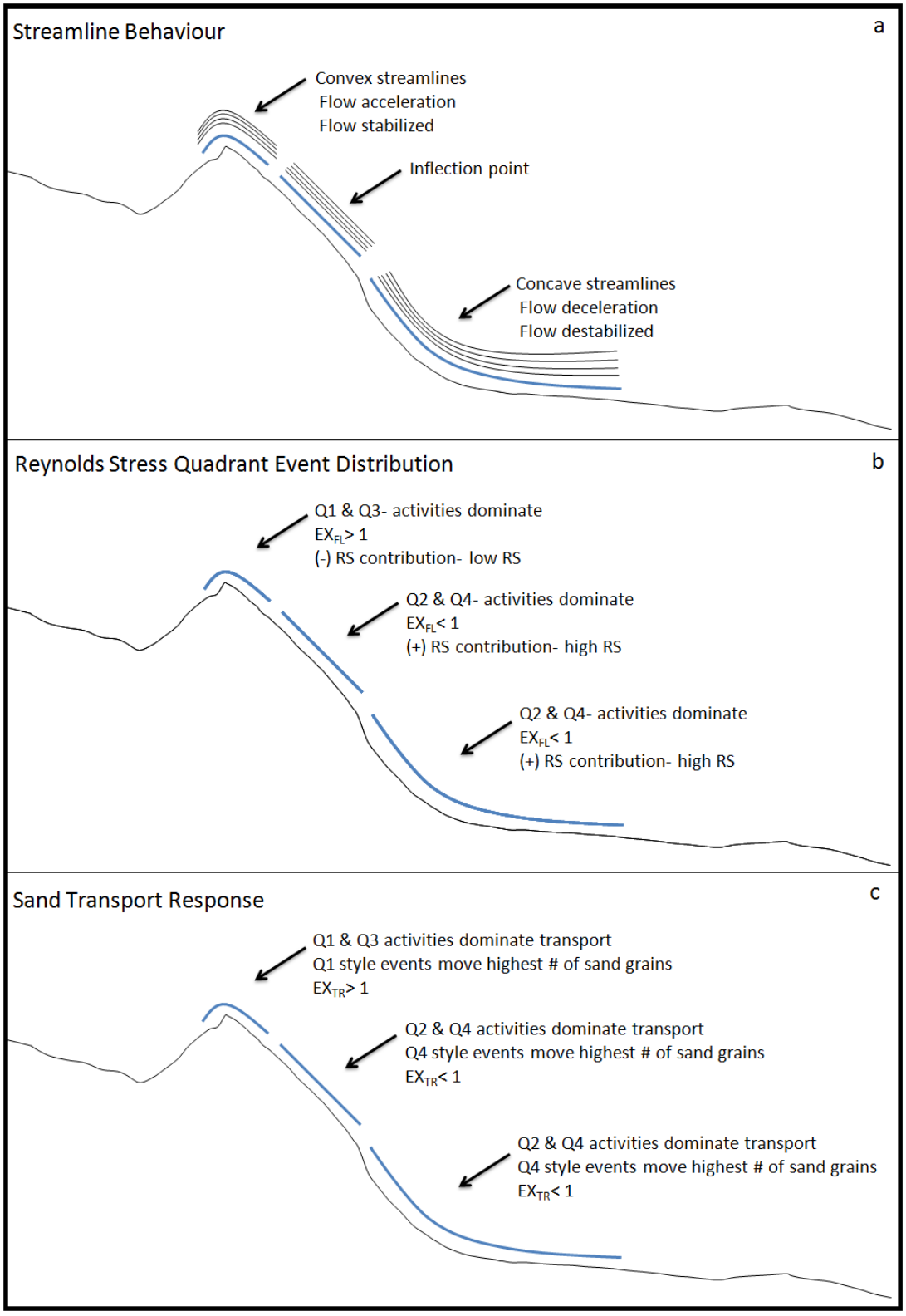

Figure 3.8: Schematic diagram describing the streamline behaviour, Reynolds stress quadrant activity distribution and sand transport responses at different locations over a foredune.

3.6.3. Morphodynamic Implications

The greatest frequency of Q2 ejection and Q4 sweep activities and the highest values of RS occurred at the beach, toe, and stoss locations. Others have stated that sediment entrainment and transport potential may be highest in these locations, which would allow for sediment supply to the foredune (e.g., Hesp et al., 2005; Walker et al., 2006; Walker et al., 2009b; Chapman et al., in preparation, Section 2.0). Results presented here show that the highest transport activity occurs at the beach and toe compared to the stoss. Q4 sweep activities dominate sand transport at the beach, toe, and stoss locations suggesting that positive streamwise velocity fluctuations (+u') and negative vertical velocity fluctuations (-w') have a greater potential for entraining and transporting sediment to the foredune than Q2 ejection activities (Table 3.2). At the crest of the dune there is a shift toward Q1 outward and Q3 inward interactions driving sand transport despite a coincident decrease in RS, which suggests a decrease in sand transport potential and possible deposition to occur. Q1 outward interactions dominate sand transport in the crest region suggesting that both positive streamwise and vertical velocity fluctuations (+u' and +w') have greater potential for entraining and transporting sediment at the crest and into the lee, despite observed declines in RS in this region, which in theory, suggests deposition. Though site specific, the beach and toe experienced the largest amount of sand transport compared to the stoss and crest during alongshore flow. The beach and toe had roughly 2 to 3 orders of magnitude more sand grains moved than the stoss and crest, suggesting that alongshore flows may be the most component in moving sand to the dune toe, due to long fetch lengths (Arens, 1996; Bauer et al., 2009). The crest and stoss had the greatest number of sand grains moved during obliquely

onshore flow. The crest experienced greater sand transport than the stoss and was driven by outward interactions and low time-averaged RS indicating that sand transport can occur during all different RS conditions.

3.7. Conclusion

This study provides novel information on turbulent airflow behaviour, Reynolds stress patterns and related turbulent quadrant activity distributions, and resulting sand transport patterns over a foredune. Reynolds stress decomposition was used to quantify and examine the spatial behaviour of quadrant activities responsible for near surface stress generation and resulting sand transport. From this, implications for sand transport pathways/mass balance, etc. and dune morphodynamics are discussed. The main conclusions are:

1. Topographic forcing is a driving factor in the distribution of turbulent activities responsible for near-surface stress generation over the dune. Increased near-surface Reynolds stress at the beach, toe, and stoss region enhances the frequency of stress generating Q2 ejection and Q4 sweep activity. Reynolds stresses were highest in the near-parallel flow above the stoss slope, where Q2 ejection and Q4 sweep activity frequencies were high and flow exuberance values were low. At the crest Reynolds stresses decrease due to increasing frequencies of Q1 and Q3 interaction activity, which contribute negatively to stress generation. Although data presented here were measured at a relatively coarse temporal resolution (1 Hz), these results confirm the ‘flow exuberance effect’ identified by a companion study at the same site.

2. A ‘transport exuberance effect’ is identified that controls the spatial distribution of quadrant activities responsible for sand transport over the foredune. Q2 ejection and Q4 sweep activities (that contribute positively to RS generation) drive sand transport at the beach, toe, and stoss locations and were responsible for >60% of observed sand transport at these locations during a 30 minute run. Related to the flow exuberance effect, this reflects transport activities associated with stress-generating turbulent activities that are forced by concave streamline curvature over the lower dune. Dominance of Q4 sweeps in transport events at these locations suggests that positive streamwise velocity fluctuations (+u’) and negative vertical velocity fluctuations (-w’) have a greater potential for entraining and transporting sediment to the foredune than Q2 ejection activities. At the crest, there is a shift to transport activities associated with stress-reducing Q1 and Q3 interaction activities, which are responsible for 79 to 88% of observed transport activity. Outward (Q1) interactions dominate sand transport in the crest region suggesting that both positive streamwise and vertical velocity fluctuations (+u’ and +w’) assist in entraining and transporting sediment despite observed declines in RS at this location. Although observed w’ values are lower than streamwise (u’) fluctuations, this research shows that vertical velocity contributions to the aeolian transport process over dunes may be more significant than previously thought.
3. Site specific, sand transport at the beach and toe was roughly 2 to 3 orders of magnitude greater than sand transport at the stoss and crest during alongshore flow. Alongshore flows were competent at moving large amounts of sand grains

over the beach (compared to the stoss and crest), which are potentially deposited by the toe to infill scarps, create ramps, and later be transported to the stoss and crest. The stoss and crest have larger amounts of sand transport during obliquely onshore flow with the crest having a greater amount of sand transport than the stoss. Sand transport at the crest is driven by outward interactions and has a low time-averaged RS indicating that sand transport can occur during all different RS conditions.

3.8. Acknowledgements

This research was supported by Parks Canada Ecosystem Science Fund support from Greenwich Dunes, PEI National Park, Natural Sciences and Engineering Research Council (NSERC) Discovery grants to IJW and RDA, Canada Foundation for Innovation (CFI) Research Infrastructure Grant to IJW, and National Science Foundation of America funding to PAH, New Brunswick Innovation Foundation grant to JO. Valuable field assistance was provided by Rhiana Bams from Mount Allison University, Sackville, NB and Parks Canada Agency staff Allan McGowan.

4.0 Conclusion

4.1. Discussion and Conclusions

This thesis provides new information on turbulent airflow, near-surface Reynolds stress and correlations between quadrant activity distributions and sand transport over a coastal foredune. Reynolds stress decomposition of turbulent velocity measurements was used to examine and quantify patterns in quadrant activities responsible for near-surface stress generation and sand transport at several locations over the beach-dune system. The thesis is structured as two research papers (Sections 2.0 and 3.0) that will be submitted to peer-reviewed journals for publication. Data for this research was obtained from two different field experiments (2004 and 2010) over the same stretch of vegetated foredune at the Greenwich Dunes, Prince Edward Island, Canada. The introductory Section 1.0 sets the context for the research by providing a comprehensive literature review. Section 2.0 examines high-frequency (32Hz) measurements of three-dimensional turbulent velocity and Reynolds Stress (RS) behaviour at four locations and two different sample heights over a vegetated foredune at Greenwich Dunes, Prince Edward Island, Canada. The specific objectives of this section are: i) to measure and describe high-frequency variations in turbulent velocity components (u, v, w) at two different heights and four different locations over the foredune; ii) to quantify and examine patterns in, and properties of, airflow dynamics and decomposed turbulent Reynolds stress signals (e.g., ejections, sweeps, inward/outward interactions) that drive surface stress generation with a goal of improving understanding of aeolian sand transport process over foredunes; and iii) to interpret interactions between turbulent flow, topographic forcing effects (e.g.,

streamline curvature and compression) and dune position, iv) to discuss implications for dune morphodynamics.

The purpose of Section 3.0 is to quantify and explore coarser scale (1 Hz) interactions between turbulent airflow behaviour, Reynolds stress signal distributions, and observed sand transport over a vegetated foredune. Specific research objectives include: i) to measure variations in quasi-instantaneous (1hz) turbulent velocity components (u ,v, w), RS distributions and activities, and co-located sand transport intensity (grain counts) along a transect over a vegetated foredune; ii) to quantify and examine relationships between near-surface airflow, decomposed RS activities (e.g., ejections, sweeps, inward/outward interactions) responsible for stress generation, and coincident sand transport; and iii) to explain patterns in near-surface airflow dynamics, Reynolds stress activity distributions, and observed sand transport, and iv) to discuss implications for sand supply and transport patterns over a vegetated foredune.

Section 2.0 shows that topographic forcing of airflow over a foredune influences the distribution of RS and related quadrant activity distributions. Increased near-surface Reynolds stress at the toe and lower stoss region enhances the frequency of stress generating Q2 ejection and Q4 sweep activity. Reynolds stresses were highest in near-parallel flow above the stoss slope, where Q2 and Q4 activity frequencies were high and flow exuberance values ($Exuberance_{Flow}(EX_{FL}) = \frac{Quadrant\ 1+Quadrant\ 3}{Quadrant\ 2+Quadrant\ 4}$) were low. At the crest, despite flow acceleration in this region, Reynolds stresses decrease due to increasing frequencies of Q1 and Q3 interaction activity, which contribute negatively to stress generation.

Changes in incident flow angle and speed affect turbulent flow properties and RS distribution over the foredune. As flow angles become more onshore (by 13° to 22°) resultant speed along the stoss and at the crest increases, whereas a decrease in observed at the toe and lee of the dune. Reynolds stresses at the toe and lower stoss increase as incident flow becomes more onshore and as resultant speed increases, whereas, at upper stoss, crest, and lee locations RS decreases. As Reynolds stresses increased there was an increase in Q2 (ejections) and Q4 (sweeps) activities. When RS decreased there was a decrease in Q2 (ejections) and Q4 (sweeps) activities and a noticeable increase in Q1 (outward interactions) and Q3 (inward interactions) activities.

Finally, section 2.0 reveals a flow exuberance effect over the foredune, which controls the RS and related quadrant activities spatial distribution. Q2 ejection and Q4 sweep activities that contribute positively to RS generation were the most frequent at the toe and stoss locations. This reflects the concave streamline curvature over the lower dune and the conveyance of these stress-generating activities. Toward the crest these stress-generating activities decline in frequency to increasing Q1 and Q3 interaction activities. This decline suggests a decrease in sand transport potential and an increase for sand deposition toward the crest. The flow exuberance effect was enhanced for more onshore flow angles suggesting an increase for potential sand entrainment and transport over (and beyond) the dune.

Section 3.0 builds on the findings of section 2.0 and shows that quadrant activity distributions and the flow exuberance effect have important implications for sand transport over dunes. It shows that topographic forcing is a driving factor in the distribution of turbulent activities responsible for near-surface stress generation over the

dune. Increased near-surface Reynolds stress at the beach, toe, and stoss region enhances the frequency of stress generating Q2 ejection and Q4 sweep activity. Reynolds stresses were highest in the near-parallel flow above the stoss slope, where Q2 ejection and Q4 sweep activity frequencies were high and flow exuberance values were low. At the crest Reynolds stresses decrease due to increasing frequencies of Q1 and Q3 interaction activity, which contribute negatively to stress generation. Although data presented here were measured at a relatively coarse temporal resolution (1 Hz), these results confirm the 'flow exuberance effect' identified by a companion study at the same site.

Although measured here at a relatively coarse temporal resolution (1 Hz), these results confirm the 'flow exuberance effect' identified in section 2.0. Results identify a 'transport exuberance effect' that controls the spatial distribution of quadrant activities responsible for sand transport over the foredune. Q2 ejection and Q4 sweep activities (that contribute positively to RS generation) drive sand transport at the beach, toe, and stoss locations and were responsible for >60% of observed sand transport at these locations during a 30 minute run. Related to the flow exuberance effect, this reflects transport events associated with stress-generating turbulent activities that are forced by concave streamline curvature over the lower dune. Dominance of Q4 sweeps in transport events at these locations suggests that positive streamwise velocity fluctuations (+u') and negative vertical velocity fluctuations (-w') have a greater potential for entraining and transporting sediment to the foredune than Q2 ejection activities. At the crest, there is a shift to transport events associated with stress-reducing Q1 and Q3 interactions, which are responsible for 79 to 88% of observed transport activity. Outward (Q1) interactions dominate sand transport in the crest region suggesting that both positive streamwise and

vertical velocity fluctuations (+u’ and +w’) assist in entraining and transporting sediment despite observed declines in RS at this location.

Although observed w’ values are lower than streamwise (u’) fluctuations, this research shows that vertical velocity contributions to the aeolian transport process over dunes may be more significant than previously thought. Finally it was acknowledged that, though site specific, sand transport at the beach and toe was roughly 2 to 3 orders of magnitude greater than sand transport at the stoss and crest during alongshore flow. Alongshore flows were competent at moving large amounts of sand grains over the beach (compared to the stoss and crest), which are potentially deposited by the toe to infill scarps, create ramps, and later be transported to the stoss and crest. The stoss and crest have larger amounts of sand transport during obliquely onshore flow with the crest having a greater amount of sand transport than the stoss. Sand transport at the crest is driven by outward interactions and has low time-averaged RS indicating that sand transport can occur during all different RS conditions.

4.2. Limitations of Datasets

Section 2.0 and Section 3.0 data sets were both extremely rich, though each had their own limitations. The data set utilized for section 2.0 had three-dimensional turbulent airflow collected at an exceptionally high frequency (32 Hz) for the aeolian field, making it extremely rich. One of the biggest limitations of this dataset was sediment transport was not measured. Though measuring sediment transport was not the primary goal of this experiment it would have enhanced the interpretations immensely. Another limitation of this dataset was the behaviour of the flow. For this data set it would have been ideal to

have directly onshore winds, instead the winds were alongshore, though had a consistent velocity greater than the sediment transport threshold.

The data set utilized for section 3.0 had three-dimensional turbulent airflow collected at a coarser frequency than section 2.0 (1 Hz), but also had instantaneous sediment transport measurements (1 Hz). One of the biggest limitations to this dataset was the consistency of working instrumentation during onshore flow. Unfortunately during this experiment several of the instruments malfunctioned during the onshore flow, leaving gaps of missing data over the foredune. Another limitation of this dataset was the flow behaviour, where the majority of the flow was offshore and alongshore. When the flow finally shifted to onshore the instrumentations started to malfunction. Through understanding these limitations it enhances the design of the next experiment, though it is recognized that flow behaviour cannot be controlled.

4.3. Research Contributions and Future Directions

The major contribution of this research is the identification of near-surface Reynolds stress distribution and sand transport over a vegetated foredune. There have been a few attempts at characterizing and quantifying turbulent flow activities in an aeolian setting using the Reynolds stress decomposition method (Baddock et al. 2011; Wiggs and Weaver, in review), whereas, the fluvial and meteorological settings have had some success (e.g., Jackson, 1976; Drake et al., 988; Robert et al, 1996; Best and Kostaschuk, 2002; Roy et al., 2004) (e.g., Lu and Willmarth, 1973; Lee and Black, 1993; Yue et al., 2007; Finnigan et al., 2009; Mazumder et al., 2009; Nemitz et al., 2009; Nemitz et al., 2009). Through the examination of the near-surface Reynolds stress it was

recognized that topographic forcing has a large influence on the distribution of Reynolds stress and quadrant activities. From here it was identified that there was a flow exuberance effect which describes the spatial distribution of Reynolds stress and related quadrant activities. The relationship between quadrant activity distribution and sand transport revealed a transport exuberance effect, which describes what quadrants are dominating the sand transport over the dune at a given point. It was recognized that the positive streamwise fluctuating velocity component (+u`) and the vertical fluctuating velocity component were responsible for the majority of the sand transport. This provides a basis to the role that vertical velocity plays in sand transport and through more exploration it will aid in the explanation to location of sediment entrainment, transport, and deposition over a foredune.

This thesis challenges currents views in aeolian research, especially the view that streamwise motions dominate the sand transport over dunes. The research presented above illustrates that the positive streamwise fluctuating velocity component (+u') and the vertical fluctuating velocity component(w') may play a greater role than initially recognized. Due to this, there is a need to obtain a greater understanding of the role that the vertical velocity component (w) plays in turbulent flow and sand transport over a dune. Overall, decomposed Reynolds stress method may offer an explanation of turbulent flow and sand transport over the foredune; however, it is not possible to explain this only using time averaged values. Additional research into the patterns of quadrant activities and Reynolds stresses is required, especially prior to an activity transporting sand which may help clarify the process of sand entrainment, transportation, and deposition.

It is still unclear as to where there sediment is being entrained and deposited. This research allowed for a examination of instantaneous sand transport, providing information on the amount of sand grains moved per second and what type of momentum exchange the surface is experiencing (e.g., positive or negative momentum exchange). A greater amount of information needs to be collected on the location of entrainment and deposition and possible from the surface stresses that are contributing to the entrainment locations. From here sand pathways and mass balance needs to be investigated.

5.0 References

Anderson, J.L. and Walker, I.J., 2006. Airflow and sand transport variations within a backshore-parabolic dune plain complex: NE Graham Island, British Columbia, Canada. Geomorphology, 77: 17-34.

Arens, S.M., 1996. Patterns of sand transport on vegetated foredunes. Geomorphology, 17: 339-350.

Baas, A. C. W., 2006. Wavelet power spectra of aeolian sand transport by boundary layer turbulence. Geophysical Research Letter, 33, L05403, doi:10.1029/2005GL025547.

Baddock, M.C., Wiggs, G.F.S., and Livingstone, I., accepted 2011. A field study of mean and turbulent flow characteristics upwind, over and downwind of barchan dunes. Earth Surface Processes and Landforms.

Bauer, B.O., Davidson-Arnott, R.G.D., Hesp, P.A., Namikas, S.L., Ollerhead, J., and Walker, I.J., 2009. Aeolian sediment transport conditions on a beach: Surface moisture, wind fetch, and mean transport rates. Geomorphology, 105: 106-116.

Bauer, B.O., Davidson-Arnott, R.G.D., Hesp, P.A., Namikas, S.L., Ollerhead, J., and Walker, I.J., 2009. Aeolian sediment transport on a beach: Surface moisture, wind fetch, and mean transport. Geomorphology, 105: 106-116.

Bauer, B.O., Yi, J., Namikas, S.L., and Sherman, D.J., 1998. Event detection and conditional averaging in unsteady aeolian systems. Journal of Arid Environments, 39: 345-375.

Best, J. L., 1993. On the interactions between turbulent flow structure, sediment transport and bedform development: some considerations from recent experimental research, in Word, N. J., French, J. R. and Hardisty, J. (as), Turbulence: Perspectives on Flow and Sediment Transport, John Wiley & Sons, Chichester, 61-92.

Best, J.L. and Kostaschuk, R.A. 2002. An experimental study of turbulent flow over a low-angle dune. Journal of Geophysical Research, 107: 929-955.

Butterfield, G.R., 1991. Grain transport in steady and unsteady turbulent airflows. Acta Mech. (suppl.), 1: 97-122.

Chapman, C., Walker, I.J., Bauer, B.O., Hesp, P.A., and Davidson-Arnott, R.D.G.,(unpublished). Turbulent Reynolds stress and quadrant activities in wind flow over a vegetated foredune.

Davidson-Arnott, R.G.D. and Bauer, B.O., 2009. Aeolian sediment transport on a beach: Thresholds, intermittency, and high frequency variability. Geomorphology, 105: 117-126.

Davidson-Arnott, R.G.D., Bauer, B.O., Walker, I.J., Hesp, P.A., Ollerhead, J., and Delgado-Fernandez, I., 2009. Instantaneous and mean aeolian sediment transport rate on beaches: An intercomparison of measurements from two sensor types. Journal of Coastal Research, SI56: 297-301.

Davidson-Arnott, R., Ollerhead, J., and Walker, I.J., 2007. Annual variations in the beach and foredune system, Greenwich Dunes, Prince Edward Island National Park. Parks Canada Final Report (PEI-2002-01R), June 30, 2007.

Davidson-Arnott, R.G.D., Yang, Y., Ollerhead, J., Hesp, P.A., and Walker, I.J., 2008. The effects of surface moisture on aeolian sediment transport threshold and mass flux on a beach. Earth Surface Processes and Landforms, 33: 55-74.

Delgado-Femandez, I. and Davidson-Arnott, R.D.G., 2011. Meso-scale aeolian sediment input to coastal dunes: The nature of aeolian transport events. Geomorphology, 126: 217- 232.

Drake, T.G., Shreve, R.L., Dietrich, W.E., Whiting, P.J., and Leopold, L.B., 1988. Bedload transport of fine gravel observed by motion-picture photography. Journal of Fluid Mechanics, 192: 193-217.

Finnigan, J.J., Shaw, R.H., Patton, E.G., 2009. Turbulence structure above a vegetation canopy. Journal of Fluid Mechanics, 637: 387-424.

Hesp, P.A., 2002. Foredunes and blowouts: initiation, geomorphology and dynamics. Geomorphology, 48: 245-268.

Hesp, P.A., 1988. Morphology, dynamics, and internal stratification of some established foredunes in southeast Australia. In: P. Hesp and S.G. Fryberger (Editors), Eolian Sediments. Sedimentary Geology, 55: 17-41.

Hesp, P.A., 1983. Morphodynamics of incipient foredunes in New South Wales, Australia. In: M.E. Brookfield and T.S. Ahlbrandt (Editors), Eolian Sediments and Processes, Elsevier, Amsterdam, pp. 325-342.

Hesp, P.A., Davidson-Arnott, R.G., Walker, I.J., and Ollerhead, J., 2005. Flow dynamics over a vegetated foredune at Prince Edward Island, Canada. Geomorphology, 65: 71-84.

Hesp, P.A., Walker, I.J., Namikas, S.L., Davidson-Arnott, R.G.D., Bauer, B.O., and Ollerhead, J., 2009. Storm wind flow over a foredune, Prince Edward Island, Canada. Journal of Coastal Research, SI56: 312-316.

Jackson, P.S. and Hunt, J.C.R., 1975. Turbulent wind flow over a low hill. Q. J. R. Meteorol. Soc. 101, 929-955.

Jackson, R. G., 1976. Sedimentological and fluid-dynamic implications of the turbulent bursting phenomenon in geophysical flows. Journal of Fluid Mechanics, 77: 531-560.

Kostaschuk, R., Shugar, D.H., Best, J.L., Parsons, D.R., Lane, S.N., and Hardy, R.J., 2008. Suspended sediment transport over a dune. In: Parsons, D.R., Best, J.L., and Garlan, T.

(Editors), Marine Sand-wave and River Dune Dynamics III. University of Leeds, UK, pp.197-201.

Kostaschuk, R., Shugar, D.H., Best, J.L., Parsons, D.R., Lane, S.N., Hardy, R.J., and Orfeo, O., 2009. Suspended sediment transport and deposition over a dune: Rio Parana, Argentina. Earth Surface Processes and Landforms, 34: 1605-1611.

Landcaster, N., Nickling, W.G., and McKenna Neuman C.K., and Wyatt, V.E., 1996. Sediment flux and airflow on the stoss slope of a barchan dune. Geomorphology, 17: 55-62.

Lee, X., and Black, T.A., 1993. Atmospheric turbulence within and above a Douglas-fir stand. Part 1: Statistical Properties of the velocity field. Boundary-Layer Meteorology, 64: 149-174.

Livingston, I., Wiggs, G.F.S., and Weaver, C.M., 2007. Geomorphology of desert sand dunes: A review of recent progress. Earth- Science Reviews, 80: 239-257.

Lu, S.S. and Willmarth, W.W., 1973. Measurements of the structure of the Reynolds stress in a turbulent boundary layer. Journal of Fluid Mechanics, 60: 481-511.

Lynch, K., Jackson, D.W.T., and Cooper, J.A.G., 2009. Foredune accretion under offshore winds. Geomorphology, 105: 139-146.

Mazumder, B.S., Pal, D.K., Ghoshal, K., and Ojha, S.P., 2009. Turbulence statistics of flow over isolated scalene and isosceles triangular-shaped bedforms. Journal of Hydraulic Research, 47: 626-637.

Nemitz, E., Hargreaves, K.J., Neftel, A., Loubet, B., Cellier, P., Dorsey, J.R., Flynn, M., Hensen, A., Weidinger, T., Meszaros, R., Horvath, L., Dammgen, U., Fruhauf, C., Lopmeier, F.J., Gallagher, M.W., and Sutton, M.A., 2009. Intercomparison and assessment of turbulent and physiological exchange parameters of grassland. Biogeosciences, 6: 1445-1466.

Nemitz,E., Loubet, B., Lehmann, B.E., Cellier, P., Neftel, A., Jones, S.K., Hensen, A., Ihly, B., Tarakanov, S.V., and Sutton, M.A., 2009. Turbulence characteristics in grassland canopies and implications for tracer transport. Biogeosciences, 6: 1519-1537.

Nield, J.M., and Baas, A.C.W., 2008a. Investigating parabolic and nebkha dune formation using a cellular automaton modelling approach. Earth Surface Processes and Landforms, 33: 724-740.

Nield, J.M., and Baas, A.C.W., 2008b. The influence of different environmental and climatic conditions on vegetated aeolian dune landscape development and response. Global and Planetary Change, 64: 76-92.

Oke., T.R., 1978. Boundary Layer Climates. Methuen, New York.

Ollerhead, J., Davidson-Arnott, R., Johnston, P., Walker, I., and Hesp, P., 2003. Seasonal variations in a beach and foredune system, Greenwich Dunes, Prince Edward Island National Park. Canadian Coastal Conference 2003.

Ollerhead, J., Davidson-Arnott, R., Walker, I.J., and Johnston, P., 2005. Seasonal variations in the beach and foredune system, Greenwich Dunes, Prince Edward Island National Park. Parks Canada Final Report (PEI-2002-01R), June 30, 2005.

Olson, J.S., 1958a. Lake Michigan dune development. I. Wind velocity profiles. Journal of Geology, 66:254-263.

Olson, J.S., 1958b. Lake Michigan dune development. II. Plants as agents and tools in geomorphology. Journal of Geology, 66:345-351.

Parsons, D.R., Walker, I.J., and Wiggs, G.F.S., 2004. Numerical modelling of flow structures over idealised transverse aeolian dunes of varying geometry. Geomorphology, 59: 149-164.

Pearce, K.I., and Walker, I.J., 2005. Frequency and magnitude biases in the 'Fryberger' model, with implications for characterizing geomorphically effective winds. Geomorphology, 68: 39-55.

Psuty, N.P., 2004. The coastal foredune: a morphological basis for regional coastal dune development. In: M.L. Martinez and N.P. Psuty (Editors), Coastal Dunes: Ecology and Conservation. Berlin: Springer-Verlag, pp. 11-28.

Robert, A., Roy, A.G., De Serres, B., 1996. Turbulence at a roughness transition in a depth limited flow over a gravel bed. Geomorphology, 16: 175 – 187.

Roy, A.G., Biron, P., De Serres, B., 1996. On the necessity of applying a rotation to instantaneous velocity measurements in river flows. Earth Surface Processes and Landforms, 21: 817-827.

Roy, A.G, Buffin-Belanger, T., Lamarre, H., Kirkbride, A.D., 2004. Size, shape and dynamics of large-scale turbulent flow structures in a gravel-bed river. Journal of Fluid Mechanics, 500: 1-27.

Sarre, R.D., 1989. Aeolian sand drift from the intertidal zone on temperate beach: potential and actual rates. Earth Surface Processes and Landforms, 14: 247-258.

Shaw, R.H., Tavangar, T., Ward, D.P., 1983. Structure of the Reynolds stress in the canopy layer. Journal of Climate and Applied Meteorology, 22: 1922-1931.

Sherman, D.J., 1995. Problems of scale in the modeling and interpretation of coastal dunes. Marine Geology, 124: 339-349.

Sherman, D.J. and Bauer, B.O., 1993. Dynamics of beach-dune systems. Progress in Physical Geography, 17(4): 413-447.

Short, A.D. and Hesp, P.A., 1982. Wave, beach and dune interactions in southeastern Australia. Marine Geology, 48: 259-284.

Shugar, D.H., Kostaschuk, R., Best, J.L., Parsons, D.R., Lane, S.N., Orfeo, O., and Hardy, R.J., 2010. On the relationship between flow and suspended sediment transport over the crest of a sand dune, Rio Parana, Argentina. Sedimentology, 57: 252-272.

Stout, J.E. and Zobeck, T.M., 1997. Intermittent saltation. Sedimentology, 44: 959-970.

Valyrakis, M., Diplas, P., Dancey, C.L., and Greer, K., 2010. Role of instantaneous force magnitude and duration on particle entrainmnet. Journal of Geophysical Research, 115: F02006, doi:10.1029/2008JF001247.

van Boxel, J.H., Sterk, G., Arens, S.M., 2004. Sonic anemometers in Aeolian sediment transport research. Geomorphology, 59: 131-147.

Venditti, J.G. and Bennett, S.J., 2000. Spectral analysis of turbulent flow and suspended sediment transport over fixed dunes. Journal of Geophysical Research, 105: 22035-22047.

Walker, I.J., 2005. Physical and logistical considerations of using ultrasonic anemometers in aeolian sediment transport research. Geomorphology, 68: 57-76.

Walker, I.J., Davidson-Arnott, R.G.D., Hesp, P.A., Bauer, B.O., and Ollerhead, J., 2009 a. Mean flow and turbulence responses in airflow over foredunes: New insights from recent research. Journal of Coastal Research, SI56: 366-370.

Walker, I.J., Hesp, P.A., Davidson-Arnott, R.G.D., and Ollerhead, J., 2006. Topographic steering of alongshore airflow over a vegetated foredune: Greenwich Dunes, Prince Edward Island, Canada. Journal of Coastal Research, 22: 1278-1291.

Walker, I.J., Hesp, P.A., Davidson-Arnott, R.G.D., Bauer, B.O., Namikas, S.L., and Ollerhead, J., 2009 b. Responses of three-dimensional flow to variations in the angle of incident wind and profile form of dunes: Greenwich Dunes, PEI, Canada. Geomorphology, 105: 127-138.

Walker, I.J. and Nickling, W.G., 2003. Simulation and measurement of surface shear stress over isolated and closely spaced transverse dunes in a wind tunnel. Earth Surface Processes and Landforms, 28: 1111-1124.

Walker, I.J. and Nickling, W.G., 2002. Dynamics of secondary airflow and sediment transport over and in the lee of a transverse dunes. Progress in Geomorphology, 26: 47-75.

Weaver, C.M. and Wiggs, G.F.S., 2011. Field measurements of mean and turbulent airflow over a barchan sand dune. Geomorphology, 128:32-41.

Wiggs, G.F.S., Livingstone, I., Warren, A., 1996. The role of streamline curvature in sand dune dynamics: evidence from field and wind tunnel measurements. Geomorphology, 17: 29-46.

Wiggs, G.F.S. and Weaver, C.M. (in review). Turbulent coherent flow structures and aeolian sediment transport over a barchan sand dune. Journal of Geophysical Research.

Yue, W., Meneveau, C., Parlange, M.B., Zhu, W., van Hout, R., and Katz, J., 2007. A comparative quadrant analysis of turbulence in a plant canopy. Water Resources Research, 43: W05422, doi:10.1029/2006WR005583.